HYDROLOGICAL PROCESSES
Hydrol. Process. **28**, 3574–3601 (2014)
Published online 21 June 2013 in Wiley Online Library
(wileyonlinelibrary.com) DOI: 10.1002/hyp.9885

Surface water and groundwater interactions in an extensively mined watershed, upper Schuylkill River, Pennsylvania, USA

Charles A. Cravotta III,[1]* Daniel J. Goode,[1] Michael D. Bartles,[2] Dennis W. Risser[1] and Daniel G. Galeone[1]

[1] *US Geological Survey, Pennsylvania Water Science Center, PA, USA*
[2] *US Army Corps of Engineers, Philadelphia District, PA, USA*

Abstract:

Streams crossing underground coal mines may lose flow, whereas abandoned mine drainage (AMD) restores flow downstream. During 2005–2012, discharge from the Pine Knot Mine Tunnel, the largest AMD source in the upper Schuylkill River Basin, had near-neutral pH and elevated concentrations of iron, manganese and sulphate. Discharge from the tunnel responded rapidly to recharge but exhibited a prolonged recession compared with nearby streams, consistent with rapid infiltration of surface water and slow release of groundwater from the mine complex. Dissolved iron was attenuated downstream by oxidation and precipitation, whereas dissolved CO_2 degassed and pH increased. During high flow conditions, the AMD and downstream waters exhibited decreased pH, iron and sulphate with increased acidity that were modelled by mixing net-alkaline AMD with recharge or run-off having low ionic strength and low pH. Attenuation of dissolved iron within the river was least effective during high flow conditions because of decreased transport time coupled with inhibitory effects of low pH on oxidation kinetics.
A numerical model of groundwater flow was calibrated by using groundwater levels in the Pine Knot Mine and discharge data for the Pine Knot Mine Tunnel and West Branch Schuylkill River during a snowmelt event in January 2012. Although the calibrated model indicated substantial recharge to the mine complex took place away from streams, simulation of rapid changes in mine pool level and tunnel discharge during a high flow event in May 2012 required a source of direct recharge to the Pine Knot Mine. Such recharge produced small changes in mine pool level and rapid changes in tunnel flow rate because of extensive unsaturated storage capacity and high transmissivity within the mine complex. Thus, elimination of stream leakage could have a small effect on the annual discharge from the tunnel, but a large effect on peak discharge and associated water quality downstream. Published 2013. This article is a U.S. Government work and is in the public domain in the USA.

KEY WORDS abandoned mines; acid mine drainage; mine hydrology; geochemical model; groundwater model; hydrograph analysis

Received 1 January 2013; Accepted 29 April 2013

INTRODUCTION

Problem

Extensive losses of surface water to underground mines and corresponding downstream gains of metal-laden drainage from the mines can diminish or eliminate aquatic habitat in streams draining areas developed for coal and other mineral resources (Younger and Wolkersdorfer, 2004). For example, in the humid, temperate climatic setting of the anthracite coalfield of eastern Pennsylvania, USA (Figure 1), second-order and third-order stream channels that overlie underground mines can be dry or intermittently flowing although the mines discharge large volumes of contaminated water from downstream outlets (Ash and Whaite, 1953; Ackman and Jones, 1991; Chaplin *et al*., 2007; Goode *et al*., 2011). Pyrite oxidation products in coal waste and mined rock along subsurface flow paths contribute acidity, sulphate, iron and other metals to the groundwater stored and discharged from the mines (Cravotta, 1994; Foos, 1997; Perry, 2001). Eventually, the contaminated groundwater may resurge as abandoned mine drainage (AMD) from tunnels, boreholes or fractures at topographically low points (Younger and Wolkersdorfer, 2004; Cravotta, 2008). The resurgent AMD may restore streamflow lost to the mines in upstream reaches and, in some instances, may add alkalinity to the stream water; however, the downstream quality and aquatic ecosystems can be impacted by the transport and accumulation of metals and associated contaminants (Kimball *et al*., 1994; Cravotta and Kirby, 2004; Cravotta, 2005; Caruso *et al*., 2008; Runkel *et al*., 2009; Cravotta *et al*., 2010). If the streamflow can be transmitted from headwaters downstream, by passing the mines, the stream habitat can be

*Correspondence to: Charles Cravotta, US Geological Survey, Pennsylvania Water Science Center, PA, USA.
E-mail: cravotta@usgs.gov

Published 2013. This article is a U.S. Government work and is in the public domain in the USA.

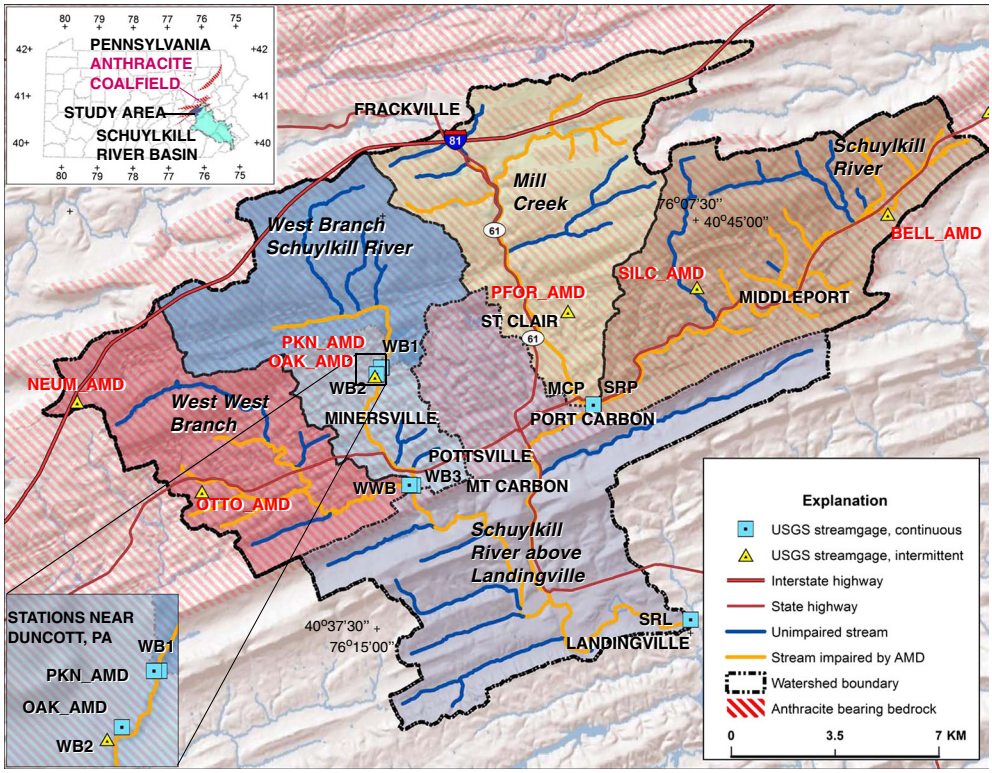

Figure 1. Drainage basins for the upper Schuylkill River and selected monitoring sites upstream of the U.S. Geological Survey (USGS) streamflow-gauging station at Landingville, PA. Drainage basins, indicated by differently colored areas, were delineated using Streamstats (Ries *et al*., 2008). Streamflow-gauging stations (blue squares) and other water-quality stations (yellow triangles) identified on the map are described in Table I. AMD-impaired stream segments are orange, whereas unimpaired streams are blue (Pennsylvania Department of Environmental Protection, 2004, 2010). Areas underlain by coal-bearing Pennsylvanian-age bedrock of the Anthracite Coalfield are indicated by red hatch symbol (Berg *et al*., 1980)

improved, the total volume of water that flows through the mines and emerges downstream as AMD can be decreased and pollutant transport within the watershed may be decreased. Nevertheless, restoring streamflow to historically dry or losing stream segments and the removal of base flow from underground mines could have unknown consequences on the flow and quality characteristics of AMD and local streams.

Hydrogeologic setting

The Schuylkill River has its headwaters in uplands of the Southern Anthracite Coalfield with altitudes exceeding 550 m above sea level and its mouth 208 km downstream, near sea level on the Delaware River at Philadelphia (Figure 1). Presently, the Schuylkill River is used for recreational fishing and boating, cooling water at thermoelectric generation facilities and drinking water to more than 1.5 million people (Schuylkill Action Network, 2006). Historically, the Schuylkill River was a primary route for the transport of anthracite from mines in the southern anthracite coalfield near Pottsville to industrial facilities in Philadelphia (Schuylkill River Heritage Area, 2010). This legacy is preserved by the names of towns in the upper Schuylkill River Basin, such as Minersville, Mount Carbon, Middleport, Port Carbon and Landingville.

The upper Schuylkill River Basin study area, which consists of the upper main stem Schuylkill River and the West Branch Schuylkill River, encompasses 340 km^2 above the US Geological Survey (USGS) streamflow-gauging station on the Schuylkill River at Landingville (Figure 1, station SRL). The long-term average annual precipitation ranges from 115 to 135 cm/year over the basin, with the greatest values for the forested uplands (National Climatic Data Center, 2012). The land cover in the basin is 74.0% forested, 9.4% commercial and residential, 4.5% agricultural, 2.8% wetlands and 9.4% mined/disturbed (Price *et al*., 2007). Some of the water bodies included as wetlands in the northern part of the watershed are large water-filled abandoned mine pits (Ash *et al*., 1949).

The anthracite coalfield in Pennsylvania (Figure 1) consists of four named coalfields in the Appalachian Mountain Section of the Ridge and Valley Physiographic Province in eastern Pennsylvania (Wood *et al*., 1986; Eggleston *et al*., 1999). Structurally, the northern, eastern middle, western middle and southern anthracite coalfields are parts of parallel, moderately to deeply downwarped

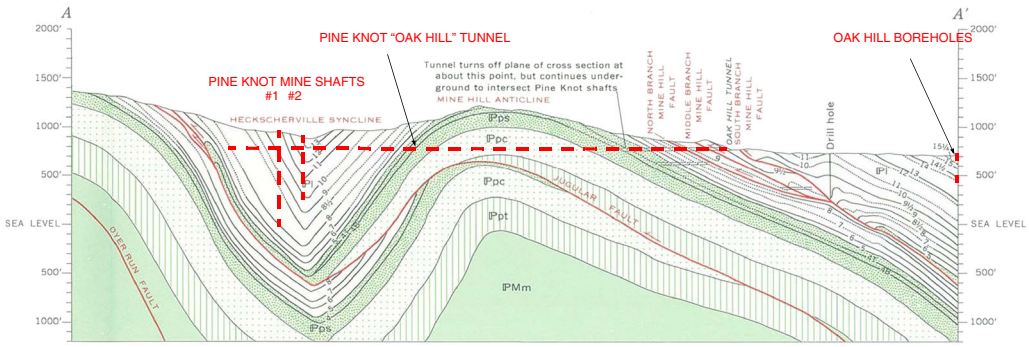

Figure 2. Structural geology of the Southern Anthracite Coalfield along the Pine Knot "Oak Hill" Tunnel, north of Minersville, PA (modified from Wood *et al*., 1968). Coalbed number and name are: 4, Little Buck Mountain; 5, Buck Mountain; 6, Seven Foot; 7, Skidmore; 8, Mammoth Bottom Split; 8 1/2, Mammoth Middle Split; 9, Mammoth Top Split; 10, Holmes; 11, Primrose; 12, Orchard; 13, Little Orchard; 14, Diamond; 14 1/2 Diamond Split; 15 Little Diamond; 15 1/4, Clinton (Wood, 1972). Numbered dashed lines indicate coal has been mined; solid lines indicate coal is unmined. No vertical exaggeration; 1,000' (feet) is approximately 300 m. Location of cross section shown on map in Figure 3

synclinoria or 'canoe-shaped' structures, with axes that generally parallel the northeast–southwest trending ridges and valleys (Figure 2). In the southern anthracite coalfield study area near Pottsville, the coal-bearing Mississippian and Pennsylvanian age rocks are exposed on the valley sides and underlie the valleys (Figure 2) (Wood *et al*., 1968, 1969; Wood, 1972; Berg *et al*., 1980). A total of 30 coalbeds have been mapped in the study area with average thicknesses from 0.3 to 4.6 m (Wood *et al*., 1968; Wood, 1972). The coalbeds are interbedded with thick (20–100 m) sequences of sandstone, siltstone, graywacke and conglomerate (Wood *et al*., 1969; Wood *et al*., 1986). Although these sedimentary host rocks locally contain calcareous clasts and cements, no limestone beds of Pennsylvanian age have been mapped in the Southern Anthracite Coalfield (Wood *et al*., 1969; Brady *et al*., 1998).

Most anthracite mines in the region were developed as large underground complexes, or 'collieries', where shafts and tunnels connected multiple coalbeds underlying the valleys. The underground mining was conducted by the 'room-and-pillar' method, with about half of the coal left to support the roof during the first stage (Eggleston *et al*., 1999). After a coalbed had been first mined, the pillars commonly were removed by retreat mining from near the mine boundary towards the mineshaft. At the mine boundaries, unmined walls of coal, or 'barrier pillars', usually were left intact to prevent explosions and fires from affecting adjacent mines and to control flooding (Figure 3). As the mines closed, the intact barrier pillars acted as underground dams, limiting the flow of groundwater to adjacent mines (Ash *et al*., 1949; Ash and Kynor, 1953).

More than 30 different underground mines, or collieries, that were active during the mid-1800s to mid-1900s (Figure 3) now are abandoned and extensively flooded by groundwater. Numerous associated surface mines, culm (waste rock and coal) banks and subsidence fractures divert overland run-off and streamflow into the underground mine pools, and hundreds of AMD sources drain from the mine pools to the Schuylkill River, West Branch Schuylkill River and tributaries (Biesecker *et al*., 1968; Cravotta *et al*., 2011). Consequently, more than 138 km of stream segments in the basin, including the West Branch Schuylkill River (36 km) and the upper main stem Schuylkill River (102 km), are 'impaired' because of AMD (Figures 1 and 3). Furthermore, after flowing from uplands to the mined area in the valleys, numerous perennial tributaries in the headwaters become intermittent because the stream channels lose water to the underground mines analogous to karst drainage systems (e.g. Freeze and Cherry, 1979). For example, the upper 6000–7000 m length of the West Branch Schuylkill River (WB1; 43.5 km^2 area), which drains approximately the same area as the Pine Knot Tunnel (Figure 1), commonly stops flowing during periods of dry weather. During these periods, AMD from the Pine Knot Tunnel and Oak Hill Boreholes constitutes nearly the entire streamflow of the lower reaches of the West Branch Schuylkill River (WB3; 62.5 km^2 area above its confluence with the West West Branch Schuylkill River) (Cravotta and Nantz, 2008).

Despite flow modification and water quality impairment because of legacy mining, Cravotta and Nantz (2008) reported that as many as 11 different fish species inhabited the streams exiting the mined part of the upper Schuylkill River Basin. All but one of these fish species were characterised as tolerant to moderately tolerant of pollution and low pH conditions. Blacknose dace (*Rhinichthys atratulus*), white sucker (*Catostomus commersoni*) and brook trout (*Salvelinus fontinalis*) of various year classes were documented at all sites surveyed. The West West Branch Schuylkill River (WWB) had the greatest diversity and numbers of fish species, reflecting better habitat and water quality than the other sites. The West Branch Schuylkill River (WB3) and Mill Creek (MCR) had the lowest species diversity and/or fewest numbers of individual fish, consistent with their degraded water quality from large inputs of AMD.

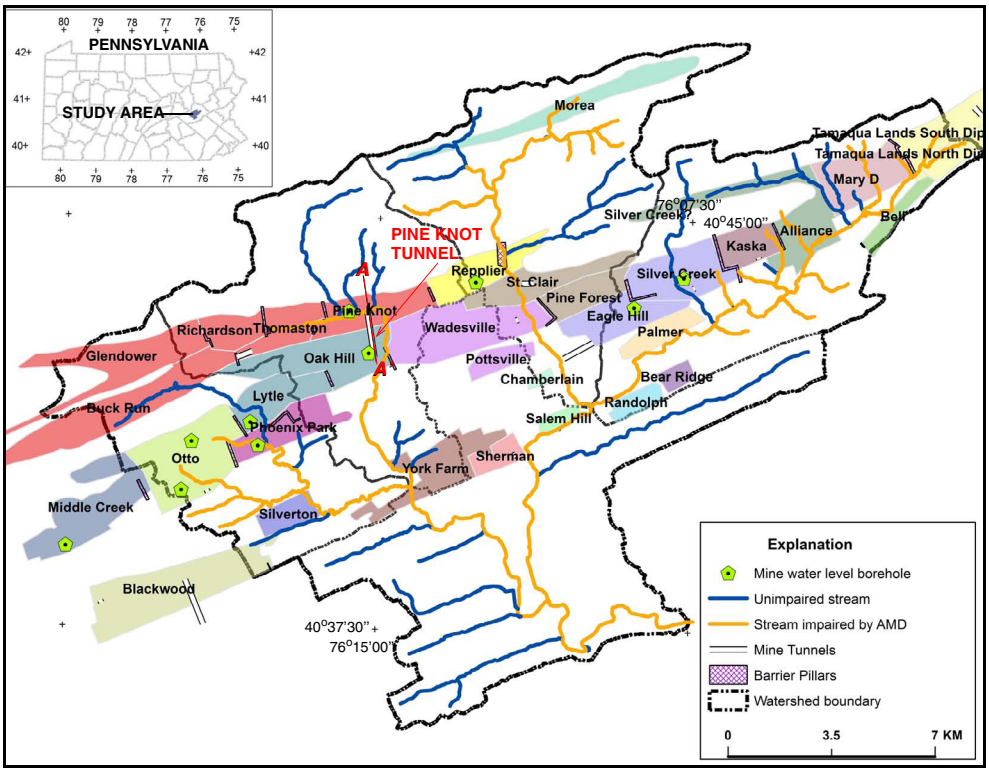

Figure 3. Approximate locations of principal mines (collieries), barrier pillars, tunnels, and associated groundwater-level data within the upper Schuylkill River Basin study area. Descriptions of collieries and "multicolliery hydrogeologic units" (MCUs) are provided in Table II. Collieries are identified by name; adjoining collieries that combine to form a MCU are identified by a continuous colored area. For example, the Pine Knot MCU, in the northwest area of the basin, consists of the Buck Run, Glendower, Richardson, Thomaston, and Pine Knot Collieries (Table II), which discharge groundwater to the Pine Knot Tunnel. Note that the Glendower and Buck Run Collieries extend beneath watershed boundaries and, thus, may facilitate the interbasin transfer of groundwater. Line A-A' indicates the approximate location of the cross section in Fig. 2

Various assessments have ranked the AMD pollution sources in the upper Schuylkill River Basin and identified strategies for remediation based on the reported flow and chemistry of the AMD (Pennsylvania Department of Environmental Protection, 2003; Cravotta *et al.*, 2011). The Pine Knot Tunnel and Oak Hill Borehole discharges, which flow to the West Branch Schuylkill River near Minersville (Figures 1, 2 and 3) and contribute approximately 30% of the annual AMD pollution to the Schuylkill River, were identified as the highest priority for clean-up. Both the Pine Knot Tunnel and Oak Hill Borehole discharges receive contributions from stream channel leakage to their underground mine sources (Cravotta and Nantz, 2008). Thus, strategies to reduce infiltration into the underground mines may be considered to maintain clean surface water in headwater streams and, possibly, to decrease the flow rates and metals loading from the mine discharges (Ash *et al.*, 1949; Goode *et al.*, 2011).

The Pine Knot Tunnel and Oak Hill Borehole discharges are only 350 m apart at their confluence with the West Branch Schuylkill River (Figures 1–3); however, they have different origins and, as explained in this paper, different hydrological and water quality characteristics. The Pine Knot Tunnel is the terminus of an extensive network of underground mine shafts and tunnels within the Pine Knot Mine complex that was constructed during the late 1800s to convey miners, equipment, coal and water from a mine level altitude of 237 m (70 m below the surface) through Mine Hill to the surface at 223-m altitude (Figures 2 and 3). After the mines closed, groundwater flooded the underground workings and rose to the tunnel level establishing the present Pine Knot mine pool. The main tunnel extends approximately 1430 m from the mine to its outlet level, after which a rock-lined channel conveys the drainage 430 m to the West Branch Schuylkill River. Along most of the length within and outside the tunnel, the drainage is in contact with the atmosphere (Murley, 2012). In contrast with the Pine Knot Mine Tunnel, the Oak Hill Boreholes were constructed in the mid-1900s to prevent the groundwater from rising to the level of roads, homes, businesses and a school in the area of Duncott. The artesian discharge from the Oak Hill Boreholes has limited contact with the atmosphere until it exits the boreholes and flows through ditches to the river that have a combined length of approximately 300 m.

METHODS

An understanding of the dynamic relations among recharge, discharge and water quality within the mined area is required to develop effective remediation strategies for large AMD sources such as the Pine Knot Tunnel and Oak Hill Boreholes. Data on the spatial and temporal variations in water quality and quantity were obtained to identify and evaluate hydrologic interactions. Conceptual and quantitative models of the physical interactions between surface water and groundwater and the hydrogeochemical processes that affect water quality were developed to indicate potential effects of mining, stream channel modification, and other activities on the upstream and downstream flow and water quality dynamics.

Hydrologic data collection and analysis

Streamflow-gauging stations for continuous monitoring of discharge were established by the USGS in 2005 at the Pine Knot Tunnel (PKN_AMD) and at upstream (WB1) and downstream (WB3) sites on the West Branch Schuylkill River and neighbouring streams, including the West West Branch (WWB), Mill Creek (MCP) and Schuylkill River (SRP), near their outlets from the mined part of the upper Schuylkill River Basin (Figure 1 and Table I). At each gauging station, a vertical staff gauge, a crest-stage gauge and a submersible, vented pressure transducer were installed to measure stream stage (water level). Additionally, in 2012, USGS installed a vented pressure transducer at the Oak Hill Boreholes and in a well into the Pine Knot Mine pool. The transducers used at the stream gauges recorded stage at a 15-min interval, whereas that in the mine pool well recorded at an hourly interval.

During 2005–2012, discharge at each gauging station was measured over a range of low-to-moderate flow conditions to develop stage-discharge ratings for each site (Rantz *et al.*, 1982). Extrapolation of stage-discharge ratings for high flow conditions was based on established ratings for nearby long-term gauging stations on the Schuylkill River at Landingville (SRL) and at Berne (SRB) (Table I). The daily average streamflow values at each gauging station for the period October 2005–September 2010 were used with the PART computer programme (Rutledge, 1998; Risser *et al.*, 2005) to estimate the annual hydrologic budget for the contributing area above the gauging station, including the percentages of total streamflow that were base flow and run-off. As explained in more detail by Risser *et al.* (2005), this estimate for annual base flow is comparable with the annual recharge to the watershed. Additionally, the length of the channel between stations (transport distance) and the relation between measured values for discharge and average velocity at the gauging stations on the West Branch Schuylkill River were used to estimate transport times between WB1, WB2 and WB3.

Table I. Streamflow gauging and water quality monitoring sites, upper Schuylkill River Basin, Schuylkill and Berks Counties, Pa.

Map ID	USGS station number	Site name	Latitude [a]	Longitude	Surface altitude (m) [b]	Drainage area (km^2) [c]
WB1	01467688	West Branch Schuylkill River ab Pine Knot Tunnel disch	404215.2	761457.5	214	43.0
WB2	01467692	West Branch Schuylkill R bl Oak Hill boreholes disch	404206.1	761507.2	212	44.4
WB3	01467752	West Branch Schuylkill River ab West West Branch	404007.6	761409.9	204	61.8
WWB	01467861	West West Branch Schuylkill River ab West Branch	404007.9	761415.4	204	47.9
MCP	01467492	Mill Cr ab Schuylkill River	404138.1	760952.6	186	65.4
SRP	01467471	Schuylkill River ab Mill Creek	404137.8	760952.0	186	69.7
SRL	01468500	Schuylkill River at Landingville	403745.0	760729.0	143	340.9
SRB	01470500	Schuylkill River at Bern	403121.0	755954.0	95	915.3
PKN_AMD	01467689	Pine Knot Disch 500-m bl tunnel	404215.2	761458.5	213	49.1
OAK_AMD	01467691	Oak Hill Disch 200-m bl boreholes	404207.6	761504.5	212	—
OTTO_AMD	403958076191401	Otto Air Shaft	403958.0	761913.0	250	—
NEUM_AMD	404134076221501	Neumeister Drift AMD Disch	404133.9	762214.3	482	—
PFOR_AMD	404320076103201	Pine Forest Mine	404320.0	761031.0	219	—
SILC_AMD	404403076072401	Silver Creek Mine Tunnel	404348.0	760726.0	259	—
BELL_AMD	404512076025501	Bell Water Level Tunnel	404510.0	760253.0	250	—

[a] Horizontal coordinate information is referenced to the North American Datum of 1983 (NAD 83). Values are degrees, minutes, seconds; 404215.2 represents 40°42'15.2" north latitude and 761457.5 represents 76°14'57.5" west longitude.
[b] Altitude referenced to the National Geodetic Vertical Datum of 1929 (NGVD 29), known as 'sea level'.
[c] Drainage area delineated using the Streamstats web application (Ries *et al.*, 2008) based on digital elevation data for the land surface topography.

Data on pH, alkalinity, acidity, concentrations of total and dissolved (0.45-μm pore size filter) metals and other water quality constituents were collected quarterly during July 2005–June 2012 at all continuous gauging stations installed in 2005 plus the Oak Hill Boreholes discharge and the West Branch below the Oak Hill Boreholes (WB2) (Table I). When samples were collected, temperature, pH, specific conductance (SC), dissolved oxygen (DO) and redox potential (Eh) were measured using a submersible sonde. Field pH and Eh were determined using a combination Pt and Ag/AgCl electrode with a pH sensor. The electrode was calibrated in pH 4.0, 7.0 and 10.0 buffer solutions and in ZoBell's solution daily when used. Values for Eh were corrected to 25 °C relative to the standard hydrogen electrode in accordance with methods of Nordstrom (1977).

The alkalinity and 'hot peroxide' acidity (hot acidity) of the unfiltered water samples were titrated using sulphuric acid (H_2SO_4) and sodium hydroxide (NaOH) to fixed end point pH values of 4.5 and 8.3, respectively (American Public Health Association, 1998a,1998b). Alkalinity of chilled samples without headspace in the bottles was measured within 8 h of sampling, whereas acidity was measured several weeks to months later at the USGS Pennsylvania Water Science Centre laboratory in New Cumberland, PA. Anion and cation analyses were conducted at the Actlabs Laboratory in Toronto, Ontario and the USGS National Water Quality Laboratory in Denver, CO (Fishman and Friedman, 1989; Crock *et al.*, 1999). Concentrations of major anions (SO_4, Cl) in 0.45-μm filtered, unpreserved subsamples were analysed by ion chromatography. Concentrations of major cations (Ca, Mg, Na, and K) and selected trace metals (Fe, Mn, Al, Ni, and Zn) in unfiltered, acidified and in 0.45-μm filtered, acidified subsamples were analysed by inductively coupled plasma optical emission spectrometry. The net acidity was calculated with the water quality data following methods of Kirby and Cravotta (2005). Hydrological data were stored in the USGS National Water Information System database (U.S. Geological Survey, 2012). Routine statistical methods were used to summarise the data and evaluate the relations among water quality constituents and flow.

Geochemical equilibrium processes (precipitation/dissolution, mixing, and mass balance) and kinetics (changes in pH and solute concentrations with transport distance and time) were considered to evaluate spatial and temporal variations in the water quality. The geochemical programme PHREEQC (Parkhurst and Appelo, 1999) was used with the WATEQ4F database (Ball and Nordstrom, 1991) and data on temperature, pH, alkalinity and dissolved solutes (0.45-μm filtered) to evaluate the equilibrium partial pressure of carbon dioxide (Pco_2), the saturation index values for various minerals and mass balance reactions to produce (1) downstream water from mixtures of upstream waters and (2) high flow water from base flow plus run-off. The Pco_2 was computed on the basis of measured pH, alkalinity and temperature. The activities of Fe^{2+} and Fe^{3+} were computed on the basis of the measured Eh, temperature and concentration of dissolved Fe (Nordstrom, 2004). The mixing proportions of the Pine Knot Tunnel, the Oak Hill Boreholes and the West Branch were estimated from measured values of flow or on the basis of 'conservative' ions such as Cl and Na. Transport times on the West Branch were estimated from the length of the channel between intermediate and downstream stations (transport distance between WB2 and WB3) and the empirical relation between measured values for discharge rate and average velocity at the downstream gauging station (WB3).

Conceptual and numerical groundwater flow model

The conceptual model for groundwater flow within abandoned anthracite mines in the study area is similar to that used by Goode *et al.* (2011) for the nearby western middle anthracite coalfield. Mine voids with high hydraulic conductivity (HK) are separated by low HK barriers of unmined coal and rock. The high HK zones consist of extensively mined coalbeds within one or more adjoining collieries that are connected to a mine shaft(s), directly or by horizontal tunnels. Where barrier pillars are intact between mined zones, adjacent collieries formed distinctive mine pools with water levels that differ by metres to tens of metres on either side of the barrier. However, if a barrier pillar between adjacent collieries is breached, the water levels in these adjoining mines tend to be uniform above the level of the breach. Where collieries are interconnected, groundwater commonly discharges from a single AMD outlet at a topographically low point within this 'multicolliery' unit (MCU) (Table II and Figure 3). Generally, the upper limit of the water level in an MCU is controlled by the altitudes of breaches in barrier pillars and/or the approximate surface altitude for the primary AMD outlet(s) in the downgradient direction.

The mine pool map of Biesecker *et al.* (1968) was the basis for the conceptual model of groundwater flow in the flooded mines of the study area. Biesecker *et al.* (1968) developed their mine pool maps after the underground mines had closed and flooded to their current extent. Their mine pool map shows the locations of the mines, elevations of effective barrier pillars and general directions of groundwater flow within the mines (Figure 4). Where water level data were not available for an abandoned mine, Ash *et al.* (1949) and Biesecker *et al.* (1968) used the altitude of the barrier pillar at the downgradient boundary of the mine to estimate the water level within the mine pool.

Published 2013. This article is a U.S. Government work and is in the public domain in the USA.

Table II. Name, estimated area, altitude of deepest mining, altitude of groundwater, and hydrologic associations of collieries in the upper Schuylkill River Basin, Schuylkill County, Pa.

Colliery name, primary	Colliery name, secondary	Colliery area (km^2)	Altitude of deepest mining (m)	Altitude of groundwater (m)	MCU name	MCU area (km^2)
Tamaqua Lands North Dip	Newkirk			263	Newkirk	11.3
Tamaqua Lands South Dip	Reevesdale	7.47	150	290	Newkirk	
Mary D		4.62	114	251	Mary D	4.6
Bell		1.48	128	252	Bell	1.5
Kaska	William	2.52	120	254	Kaska	2.5
Eagle Hill	Oakdale	3.91	−68	222	Eagle Hill	9.2
Silver Creek	Oakdale	5.29	21	247	Eagle Hill	
Palmer	Paubley	2.00	n.d.	212	Palmer	2.0
Bear Ridge	Sillman & Reed's	0.85	n.d.	204	Bear Ridge	0.9
Randolph		1.29	48	215	Randolph	1.29
Salem Hill		0.73	−21	194	Salem Hill	0.73
Pine Forest		2.94	39	220	Pine Forest	6.92
St. Clair		3.98	39	223	Pine Forest	
Pottsville		1.55	n.d.	217	Wadesville	9.28
Wadesville		7.73	−46	195	Wadesville	
Sherman		1.38	138	214	Sherman	1.38
York Farm	Black Mine	5.33	97	n.d.	York Farm	5.33
Morea	New Boston	4.97	n.d.	n.d.	Morea	4.97
Repplier	Ellsworth	3.87	126	270	Repplier	3.87
Buck Run		8.55	140	264	Pine Knot	24.95
Glendower	Taylorsville	7.07	210	314	Pine Knot	
Pine Knot	Mine Hill Gap	4.15	55	233	Pine Knot	
Richardson		2.22	113	241	Pine Knot	
Thomaston	Anchor	2.96	116	233	Pine Knot	
Lytle	Forrestville	3.66	−137	218	Oak Hill	10.15
Oak Hill	Pine Hill	6.49	−69	215	Oak Hill	
Phoenix Park	Lewis	3.81	84	232	Phoenix Park	3.81
Otto	Branchdale	7.94	−57	251	Otto	7.94
Alliance	Brockton	6.36	n.d.	n.d.	Alliance	6.81
Silver Creek?	St. Clair	0.45	n.d.	n.d.	Alliance	
Blackwood	Everet's	9.18	158	n.d.	Blackwood	9.18
Chamberlain		0.37	n.d.	n.d.	Chamberlain	0.37
Middle Creek		6.81	59	278	Middle Creek	6.81
Silverton	Black Mine	1.83	n.d.	n.d.	Silverton	1.83

MCU, multicolliery unit.

Because the Pine Knot MCU is the largest of the mine pools and the Pine Knot Tunnel is the largest AMD source in the upper Schuylkill River Basin (Figures 3 and 4), the groundwater model focused on the hydrology of this area and the Pine Knot Tunnel discharge. The groundwater model boundary delineated the area of approximately 58 km^2 that ultimately could drain to the Pine Knot Tunnel considering watershed topography and underlying interconnected mines of the Pine Knot MCU and Repplier MCU. The modelled area included the upper parts of the West West Branch, West Branch and Mill Creek watersheds and included six named underground mines or collieries covering an estimated area of approximately 29 km^2, with individual areas ranging from 2.22 km^2 for the Richardson Mine to 8.55 km^2 for the Buck Run Mine (Table II and Figure 3). The bottom altitude of the mines, obtained from the lowest gangway details shown on mine maps and reported values by Ash *et al.* (1949), ranged from 55 m above sea level for the Pine Knot Mine to 210 m above sea level for the Glendower Mine (Table II). The approximate locations of colliery boundaries and associated barrier pillars and tunnels were compiled from unpublished and published maps (Ash *et al.*, 1949; Ash and Kynor, 1953; Biesecker *et al.*, 1968) and used to create GIS files. The GIS and associated digital files on the mine locations were only approximate, because the source maps lacked coordinates and relevant projection information.

A three-dimensional groundwater flow model was developed by using MODFLOW-NWT (Niswonger *et al.*, 2011) and calibrated to the measured groundwater level in the Pine Knot mine pool and discharge at the Pine Knot

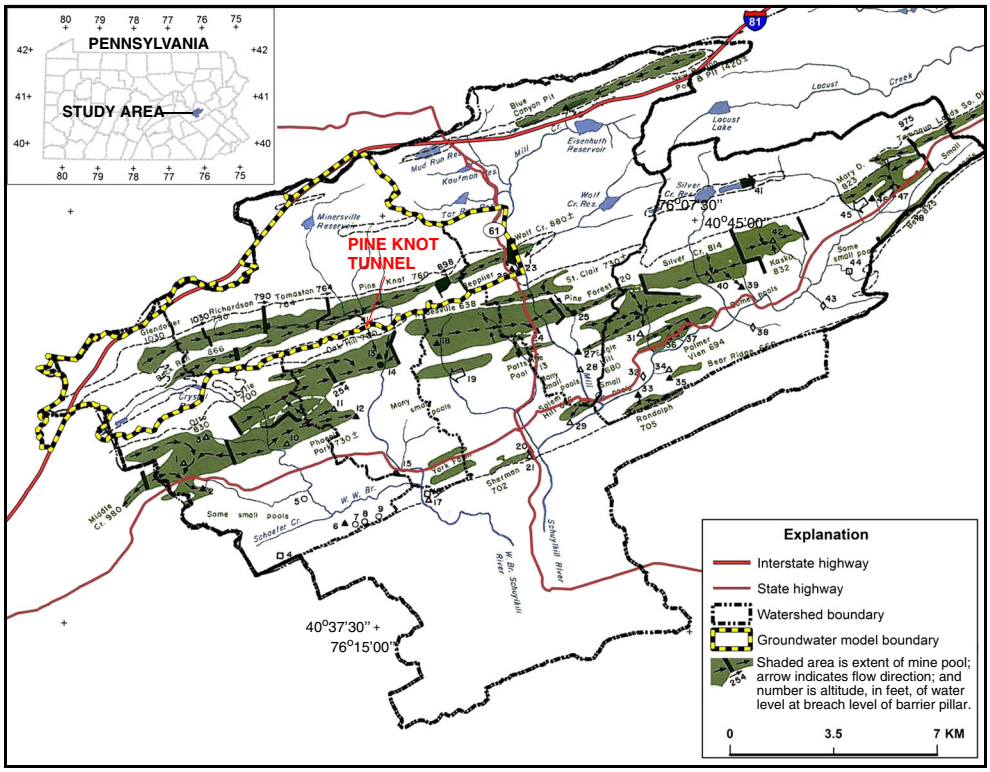

Figure 4. Underground "mine pools" as identified by Biesecker *et al*. (1968, fig. 38) and boundary for groundwater model of the Pine Knot MCU in this study. Shaded areas indicate approximate areal extent of flooded underground mines. Altitude of barrier pillar effectiveness from Ash and Kynor (1953) or altitude of mine discharge outlet generally indicates the mine pool water level

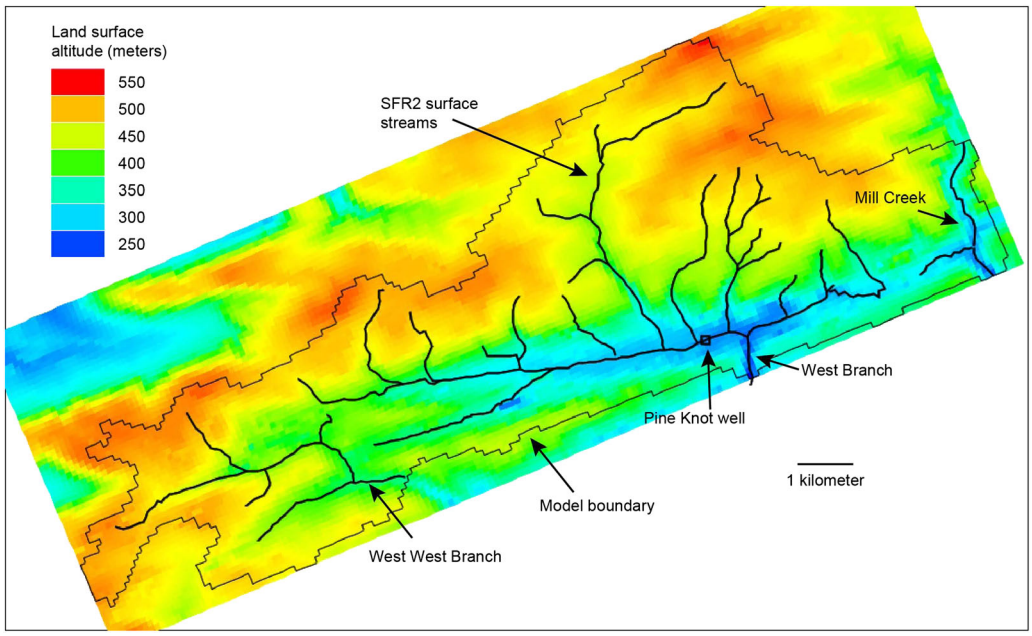

Figure 5. Land surface altitude and streams for the groundwater-flow model, and location of the water-level borehole in the Pine Knot mine pool (Figure 3)

Tunnel and the West Branch Schuylkill River above the tunnel outlet. MODFLOW-NWT is a three-dimensional finite difference model based on MODFLOW-2005 (Harbaugh, 2005) that allows automatic, improved (compared with MODFLOW-2005) drying and rewetting of model cells, an important process where the high HK mine voids desaturate overlying rocks, and where those overlying rocks may re-saturate during recharge events.

Table III. Description of layers of the groundwater flow model for the Pine Knot mine complex, upper Schuylkill River Basin, Schuylkill County, Pa.

Model layer	Layer name	Description	Thickness (m)
1	Overburden	Soil and weathered rock, stress-relief fracturing	20
2	Rock	Unweathered rock, disturbed in surface mined area	20
3	Upper mine layer	Unweathered rock and coal seams; voids in subsurface mined area	20–127 [a]
4	Lower mine layer	Unweathered rock and coal seams; voids in subsurface mined area	20–127 [a]
5	Bedrock	Unweathered bedrock	20

[a] In mined areas, the total thickness of layers 3 and 4 represents the depth of mining below layer 2, as described in the text. Each layer is one half of the total thickness.

Areas of the land surface contributing recharge to the mines were delineated by use of MODPATH for forward particle tracking (Pollock, 1994).

The model was constructed and parameterised using the ModelMuse preprocessor (Winston, 2009). The horizontal cell dimensions were 100-m square, and the model grid was aligned northeast–southwest with the regional axes of synclinal structures. The outer edges of the model were no-flow boundaries. The top of the model was the land surface, across which recharge entered the system (Figure 5). The land surface altitude was interpolated from light detection and ranging (LiDAR) elevation data accurately to 0.67 m (Pennsylvania Department of Conservation and Natural Resources, 2008). Five model layers were included, from the top: overburden, rock, upper mine, lower mine and bedrock (Table III). The overburden layer was 20-m thick and had relatively high HK due to stress relief fracturing (Wyrick and Borchers, 1981) and weathering processes. The rock layer also was 20-m thick and represented lower HK in unmined areas. An aquifer parameter zone represented the part of the rock layer in mined areas where hydraulic properties were altered by mine collapse or near-surface mining. The upper and lower mine layers had the same properties as the rock layer outside the mined area, but had distinct aquifer parameter zones within the mined areas. The total thickness of the upper and lower mine layers extended from the bottom of the rock layer to the altitude of deepest mining, or to 40 m below the rock layer, whichever was deeper. The bedrock layer was below the deepest mining, was 20-m thick and had uniform hydraulic properties. The bedrock layer corresponds to the Pottsville Formation of Mississippian and Pennsylvanian age, whereas the overlying layers in the model correspond to the Llewellyn Formation of Pennsylvanian age (Figure 2).

The void volume of the partly collapsed, partly flooded mines was modelled by aquifer parameter zones for the mined areas within the upper and lower mine layers. Using the model preprocessor, the altitude of deepest mining within the mine pool areas (Table II), corresponding to the mine pools delineated by Biesecker *et al*. (1968), was used with geologic structure contour maps to construct generalised contours of the altitude of the deepest mining. Outside the mine pool areas, the contours for the bottom of the lower mine layer were extrapolated to the valley sides, coincident with the outcrop of the Buck Mountain coalbed, which locally was the deepest economic coalbed (Figures 3, 6 and 7). The barrier pillars between the mines were simulated by including unmined rock between each mine pool, at least two model finite difference cells wide, and the rock layer over the mine layers was parameterised with an aquifer parameter zone in the area of surface mining (Figures 6 and 7). Thus, the three-dimensional model mimicked the synclinal geologic structure beneath the valley, considered actual depths and areas of mining, and included altered hydraulic characteristics for the surface and subsurface mined zones.

Simulation of groundwater flow in flooded mines is complicated by the nonlinear effects of mine barriers on flow between mine pools. As noted previously, where the water level in the mine pool is less than the altitude of the effective barrier, flow between the mines is minimal. However, very large flows can occur between the mines when the water level in the upgradient pool exceeds the effective altitude of the barrier. To approximate the dynamics of flow through a breached barrier at a particular altitude, the SFR2 package of MODFLOW was used (Niswonger and Prudic, 2005). Conduits were simulated as SFR2 'streams' in the lower mine layer (Figure 6). The altitude of the head in the conduit corresponded to the effective altitude of the barrier as reported by Ash and Kynor (1953) and Biesecker *et al.* (1968), and thus, the conduit gained flow when the groundwater level was greater than the conduit head. The conduit extended from the upgradient mine pool to the downgradient mine pool, where the conduit lost water as long as the downgradient mine pool head was less than the conduit head. When the upgradient mine pool water level was less than the head of the conduit, there was no flow across the barrier in the conduit; flow occurred at low rates through the unmined portions of the coal seams and surrounding rock.

A snowmelt recharge event in January 2012 was used to estimate aquifer properties as part of the

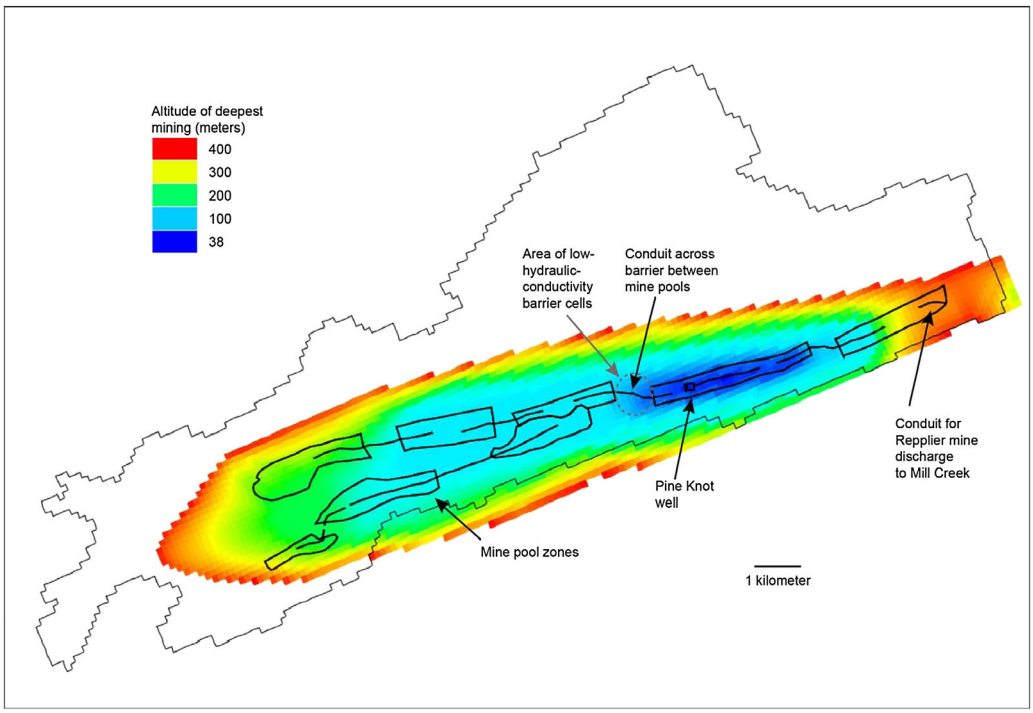

Figure 6. Mine pool zones, low hydraulic conductivity barriers, conduits for barrier breaches and altitude of deepest mining for the groundwater flow model

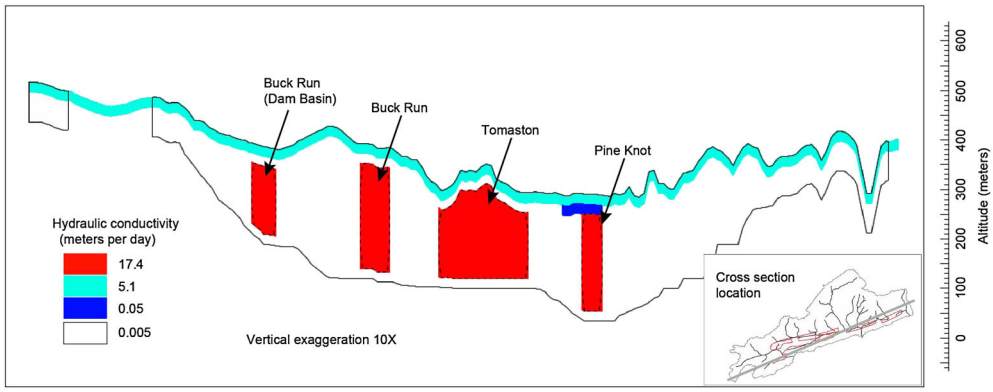

Figure 7. Cross section of the groundwater flow model showing hydraulic conductivity for mine pool zones, disturbed rock in surface mining areas, overburden, and unweathered, undisturbed rock

model calibration. The calibration simulation included four model stress periods—an initial steady-state period, a 1-day transient stress period with snowmelt recharge, a 1-day recession stress period with variable time steps and a 29-day recession stress period with constant 1-day time steps. Mine pool altitudes and discharge from the Pine Knot Tunnel and the West Branch above the Pine Knot Tunnel were used as calibration targets for the steady-state period before the recharge event. The measured altitude of the Pine Knot mine pool was heavily weighted in the calibration; other mine pool altitudes were based on the reported altitude of effective barrier pillars as indicated by Ash and Kynor (1953) and Biesecker *et al.* (1968). The measured rise and fall of the Pine Knot pool, tunnel discharge and West Branch discharge associated with snowmelt during the recharge event were used for transient calibration of HK and storage parameters and two recharge rates: one during the snowmelt event and one during recession. Six additional measurements of the Pine Knot mine pool altitude, tunnel discharge and West Branch discharge were used for the transient calibration. Automated parameter estimation used ModelMate (Banta, 2011), a preprocessor for UCODE-2005 (Poeter *et al.*, 2005),

with manual adjustments to constrain parameter values to realistic ranges and fix insensitive parameters (Hill and Tiedeman, 2007). In the parameter estimation programme, residuals (computed as the difference between observed and simulated values) in streamflow were multiplied by a weighting factor, primarily to convert discharge rates to the same units as water level measurements. The value of the weighting factor was chosen so that the sum of squared weighted residuals for the streamflow measurements was approximately the same magnitude as the sum of squared weighted residuals for water level data from the borehole in the Pine Knot mine pool (Pine Knot well).

Simulations for a high flow rainfall event in May 2012 used the calibrated model and a spatially uniform recharge rate that was assumed to equal total precipitation during the event. Hourly precipitation data obtained from a USGS weather station and three USGS stream gauges near the study area were averaged for 3-h periods. At Frackville, which is north of the study area and closer to the Pine Knot Mine than the USGS precipitation gauges, the reported daily total precipitation on 14–15 May 2012 was 1.74 and 1.91 in (4.42 and 4.85 cm), respectively (Weather Underground, Inc., 2012). These amounts were about double the average amounts of 0.84 and 1.06 in (2.13 and 2.69 cm) recorded by USGS gauges to the south. Thus, the model recharge used the temporal pattern of the USGS data, but scaled the amounts by a factor of 2 to reflect the higher daily precipitation measured at the nearest rain gauge. The effect of streamflow restoration on reducing streamflow leakage as a source of recharge to the mines was simulated by setting the vertical HK of stream segments overlying the mines to zero.

RESULTS AND DISCUSSION

Streamflow in the main tributaries exiting the mined area of the upper Schuylkill River can be described as base flow, dominated by AMD, combined with widely variable surface run-off. For example, AMD from the Pine Knot Tunnel and the Oak Hill Boreholes plus surface drainage to the West Branch above the Pine Knot Tunnel outlet (WB1) are the major sources of streamflow in the West Branch Schuylkill River downstream to its confluence with the West West Branch (Figure 1). As described later, the total streamflow of the West Branch and other sites in the study area varied temporally and spatially (Figure 8) in response to precipitation events and the infiltration and drainage characteristics of the watershed above the stream gauges. During the 2005–2012 study period, the peak discharge occurred with regional flooding during 27–29 June 2006, associated with rainfall totalling 38–48 cm in 4 days in the upper Schuylkill River Basin (National Weather Service, 2006) and during 8–9 September 2011, associated with Tropical Storm Lee and rainfall totalling 20–30 cm in 4 days (National Aeronautical and Space Administration, 2011). On the other extreme, a lack of streamflow at WB1 and low base flow conditions elsewhere (Figure 8) occurred during seasonally dry weather,

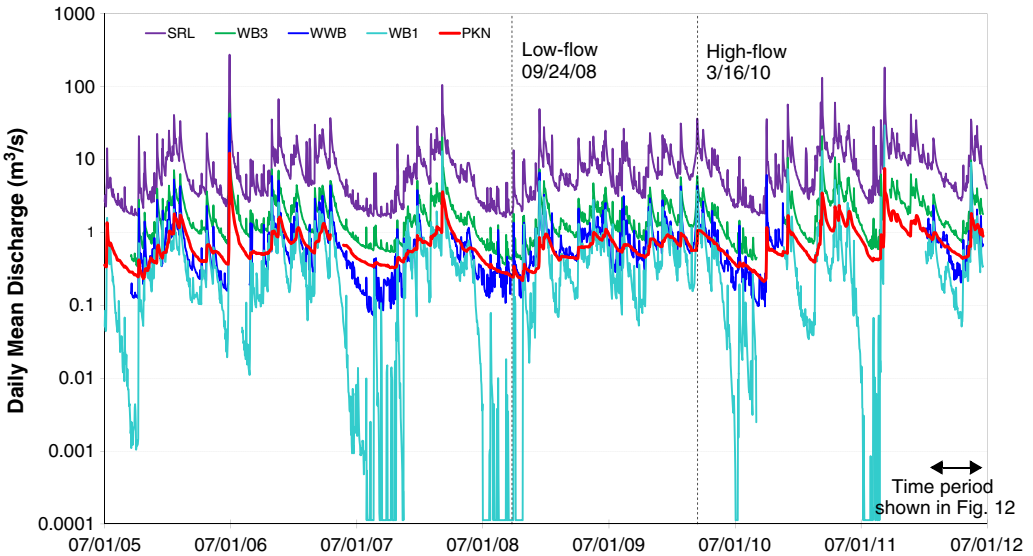

Figure 8. Daily average discharge at selected streamflow-gauging stations in the upper Schuylkill River Basin, July 2005-July 2012. SRL, Schuylkill River at Landingville; WB3, West Branch above West West Branch; WWB, West West Branch above West Branch; WB1, West Branch above Pine Knot Tunnel discharge; PKN, Pine Knot Tunnel discharge. For WB1, minimum discharge approaching 0.001 m^3/s is displayed at times when there was no flow (discharge = 0). Site descriptions and locations are in Table I and Figure 1. Vertical dashed lines indicate flow conditions for low-flow and high-flow "end-member" samples in geochemical models

Table IV. Water-quality data for Pine Knot Tunnel, Oak Hill Boreholes, and associated upper Schuylkill River Basin tributaries, Schuylkill County, Pa., July 2005 - June 2012

	01467689	01467691	01467688	01467692	01467752	01467861	01467492	01467471
	PKN_AMD	OAK_AMD	WB1	WB2	WB3	WWB	MCP	SRP
Flow (m^3/s)	0.57 (0.25/1.59)	0.18 (0.096/0.48)	0.20 (0/4.98)	0.96 (0.34/3.51)	1.20 (0.37/8.95)	0.51 (0.14/12.7)	0.68 (0.23/13.0)	0.765 (0.23/13.6)
Temp. (°C)	10.9 (9.8/11.6)	14.7 (13.9/16.4)	13.0 (1.2/25.2)	12.0 (7.5/14.6)	12.0 (5.3/16.6)	11.4 (0.7/19.3)	13.1 (2.7/19.6)	12.7 (0.9/19.2)
DO	9.9 (8.3/11.6)	2.0 (1.3/4.0)	9.4 (3.2/14.3)	9.0 (7.3/11.4)	9.5 (7.4/11.4)	9.8 (8.0/13.6)	9.9 (7.3/13.2)	9.6 (7.9/14.1)
Eh (mV)	320 (210/690)	220 (150/400)	405 (300/580)	300 (210/480)	270 (190/420)	330 (160/590)	300 (210/500)	300 (240/560)
SC (μS/cm)	570 (460/650)	1000 (860/1060)	155 (64/2450)	560 (390/740)	570 (290/730)	350 (120/600)	380 (160/530)	300 (180/440)
pH (units)	6.4 (5.3/7.3)	6.3 (5.8/7.0)	5.2 (3.9/6.8)	6.4 (5.7/6.8)	6.9 (5.6/7.2)	7.4 (6.0/8.1)	6.6 (5.5/7.3)	6.8 (5.2/7.3)
Alkalinity	34.0 (3.0/43.0)	150.0 (98.0/170.0)	2.0 (0.0/29.0)	45.0 (24.0/72.0)	46.5 (23.0/69.0)	51.5 (15.0/140.0)	11.0 (4.0/24.0)	15.5 (10.0/23.0)
Acidity	−21.5 (−29.5/−6.9)	−113 (−128/−59.4)	3.0 (−9.1/210)	−30.2 (−49.2/−12.7)	−39.5 (−59.7/−15.2)	−48.4 (−134/−12.5)	−4.0 (−20.7/5.6)	−10.9 (−17.8/−2.6)
SO_4, diss.	240 (190/320)	390 (360/450)	52 (14/1800)	210 (130/320)	190 (110/280)	110 (43/170)	120 (53/160)	120 (75/180)
Cl, diss.	17.5 (<0.1/22.0)	8.8 (5.2/11.0)	14.0 (2.6/29.0)	16.0 (0.0/22.0)	20.0 (0.0/28.0)	7.4 (0.0/16.0)	29.0 (0.0/51.0)	7.7 (4.1/24.0)
Ca, diss.	40.5 (32.0/48.0)	99.0 (72.0/110.0)	9.6 (2.8/250.0)	41.5 (23.0/66.0)	43.0 (21.0/58.0)	30.0 (12.0/57.0)	25.0 (12.0/37.0)	27.0 (17.0/42.0)
Mg, diss.	42.0 (34.0/49.0)	55.0 (49.0/61.0)	6.8 (1.7/230.0)	34.5 (20.0/52.0)	33.0 (17.0/48.0)	18.0 (6.4/32.0)	16.0 (6.2/24.0)	15.0 (10.0/24.0)
K, diss.	1.4 (0.8/1.7)	2.3 (1.6/2.9)	0.7 (0.4/1.7)	1.4 (0.9/1.8)	1.9 (1.3/2.6)	1.4 (1.0/2.3)	1.8 (0.8/2.4)	1.3 (1.1/2.2)
Na, diss.	10.0 (6.1/14.0)	32.0 (24.0/35.0)	8.0 (4.0/15.0)	14.0 (10.0/17.0)	18.0 (12.0/22.0)	11.0 (6.3/24.0)	19.0 (6.0/34.0)	7.5 (4.5/19.0)
Al, tot.	0.60 (0.40/2.60)	0.23 (0.08/0.80)	0.72 (0.40/34.00)	0.60 (0.30/1.30)	0.50 (0.29/1.10)	0.04 (<0.10/0.28)	0.76 (0.12/1.30)	0.40 (0.17/0.90)
Al, diss.	0.07 (<0.10/0.30)	0.06 (<0.10/0.30)	0.50 (<0.10/33.0)	0.04 (<0.10/0.20)	0.01 (<0.10/0.20)	0.01 (<0.10/0.12)	0.01 (<0.10/0.05)	0.01 (<0.10/0.03)
Fe, tot.	5.75 (3.40/8.60)	18.0 (13.0/21.0)	0.12 (0.05/0.66)	5.85 (3.90/12.00)	4.10 (3.20/6.10)	0.29 (0.10/1.00)	2.00 (1.10/3.20)	2.00 (1.10/2.80)
Fe, diss.	5.15 (2.80/7.00)	18.0 (12.0/21.0)	0.07 (0.05/0.50)	5.45 (3.20/10.00)	2.60 (0.91/3.20)	0.04 (0.01/0.19)	1.40 (0.17/2.70)	0.92 (0.51/1.50)
Mn, tot.	2.30 (1.70/3.10)	3.70 (3.10/4.80)	0.30 (0.12/17.0)	1.95 (1.30/2.80)	1.90 (1.10/2.70)	0.38 (0.12/0.64)	1.30 (0.61/2.00)	1.10 (0.77/1.80)
Mn, diss.	2.45 (1.70/3.00)	3.70 (3.10/4.50)	0.33 (0.12/17.0)	2.05 (1.30/3.20)	1.90 (1.10/2.80)	0.31 (0.11/0.66)	1.40 (0.61/2.00)	1.10 (0.73/1.90)
Ni, diss.	0.05 (0.04/0.07)	0.04 (0.04/0.04)	0.02 (<0.01/0.75)	0.04 (0.03/0.06)	0.03 (<0.01/0.04)	0.01 (0.01/0.02)	0.03 (<0.01/0.04)	0.03 (0.02/0.04)
Zn, diss.	0.12 (0.08/0.22)	0.05 (0.02/0.16)	0.04 (0.03/1.80)	0.08 (0.06/0.16)	0.07 (0.05/0.18)	0.02 (<0.01/0.09)	0.07 (0.03/0.11)	0.06 (0.04/0.08)

Values are median(minimum/maximum) for 24 quarterly samples; units are milligrams per liter, except as noted

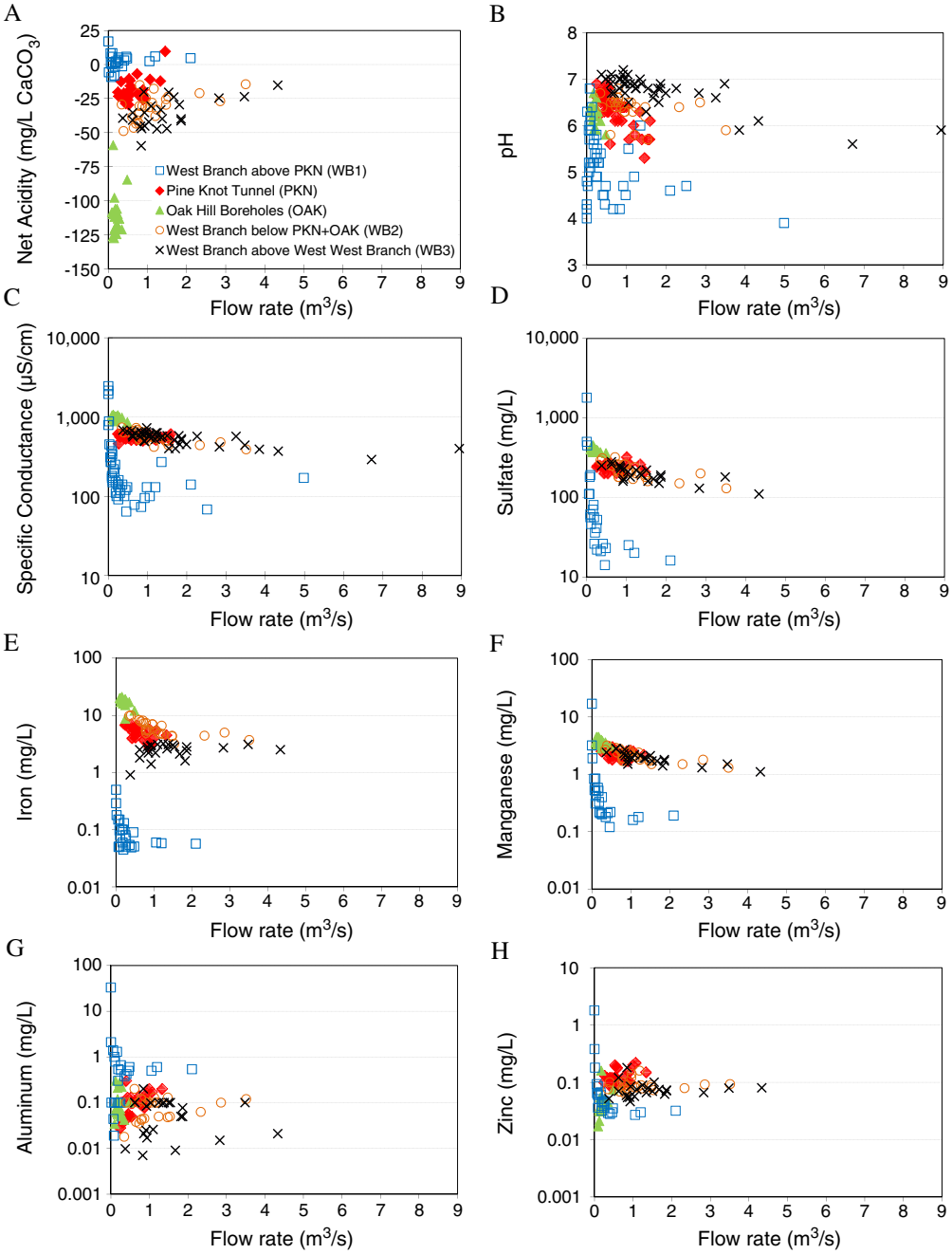

Figure 9. Relation between discharge rate and water quality of the West Branch above Pine Knot Tunnel (WB1), Pine Knot Tunnel (PKN), Oak Hill Boreholes (OAK), and West Branch below Oak Hill Boreholes at intermediate (WB2) and downstream (WB3) sites, July 2005-July 2012

July–September 2005, July–August 2007, July–October 2008, July 2010 and July–August 2011.

Water quality variations

When water quality samples were collected during the 2005–2012 study period, the flow rate of the West Branch above the Pine Knot Tunnel outlet (median 0.20 m^3/s) typically was about one third that of the Pine Knot Tunnel (median 0.57 m^3/s), but was equivalent to that of the Oak Hill Boreholes (median 0.18 m^3/s) (Table IV). Thus, the AMD from the Pine Knot Tunnel and Oak Hill Boreholes constituted the majority of streamflow during typical base flow conditions, and nearly all streamflow during seasonal low flow conditions when most, if not all, the streamflow in the upper reaches of the West Branch infiltrated to the underground mines. In contrast, during high flow conditions, surface run-off conveyed by the West Branch to WB1 frequently exceeded the combined

flows of the two AMD sources. These temporal variations in the contributions from surface water run-off and groundwater base flow had substantial effects on the downstream water quality of the West Branch and other sites studied.

Streamwater quality of the West Branch above Pine Knot Tunnel (WB1) varied from net acidic to net-alkaline (pH, 3.9–6.8; acidity, 9.1–210 mg/L); however, streamwater at the other sites was consistently net-alkaline (acidity < 0) with near-neutral pH (Table IV and Figure 9). Nevertheless, water quality degradation was indicated by elevated concentrations of iron and other dissolved metals in the water column and associated metal-rich 'ochreous' precipitate on the streambed at all the monitored stream sites. Only the WWB consistently met criteria of the Pennsylvania Department of Environmental Protection (2010) for total maximum daily loads (pH, 6.0–9.0 and concentrations of total iron < 1.5 mg/L, total manganese 1.0 mg/L and total aluminium < 0.75 mg/L) and 'criteria continuous concentration' values of the U.S. Environmental Protection Agency (2009) for protection of freshwater aquatic organisms (dissolved iron < 1.0 mg/L, dissolved aluminium < 0.087 mg/L, dissolved nickel < 0.052 mg/L and dissolved zinc < 0.12 mg/L). Although these criteria were met intermittently at most sites, the intermediate and lower reaches of West Branch (WB2, WB3) consistently were degraded by dissolved and particulate metals (Table IV). For example, during the study, concentrations of dissolved iron and manganese at West Branch near its confluence with the West West Branch (WB3) ranged from 0.91 to 3.2 mg/L and from 1.1 to 2.80 mg/L, respectively. Concentrations of dissolved aluminium rarely exceeded 0.1 mg/L at the downstream sites (Table IV) because of the limited solubility of aluminium at near-neutral pH (e.g. Nordstrom, 2004; Cravotta, 2008). Although dissolved aluminium concentrations in the West Branch above the Pine Knot Tunnel (WB1) were elevated (maximum 33.0 mg/L) in some samples with low pH (Table IV), concentrations of dissolved aluminium decreased downstream because of the rapid precipitation of aluminium hydroxide ($Al(OH)_3$) and associated solids where these waters mixed with alkaline water sources including the discharges from the Pine Knot Tunnel and Oak Hill Boreholes.

Despite attenuation of aluminium, the intermediate and lower reaches of the West Branch (WB2 and WB3) contained elevated concentrations of sulphate, iron, manganese and zinc from the Pine Knot Tunnel and the Oak Hill Boreholes (Table IV and Figure 9). During the study, the concentration of dissolved iron discharged from the Pine Knot Tunnel ranged from 2.8 to 7.0 mg/L and that at the Oak Hill Boreholes ranged from 12 to 21 mg/L, with medians of 5.15 and 18 mg/L, respectively (Table IV and Figure 9). Dissolved manganese concentrations generally were about half the values of iron. Concentrations of total dissolved solids for the Pine Knot Tunnel were composed predominantly of sulphate (190–320 mg/L), calcium (32–48 mg/L) and magnesium (34–49 mg/L), and consistently were less than half of the values for the Oak Hill Boreholes (Table IV). Nevertheless, the median iron and manganese loading rates (flow multiplied by concentration) were equivalent for these two AMD sources because the concentration of iron plus manganese for the Oak Hill Boreholes was approximately three times greater than that for the Pine Knot Tunnel, whereas the median flow rate for the Pine Knot Tunnel was approximately three times that for the Oak Hill Boreholes (Table IV).

The pH and concentration of dissolved iron decreased with increased flow rate at the Pine Knot Tunnel (Spearman's $r = -0.69$ and -0.63, respectively); however, other constituents did not vary with flow at this site (Figure 9). Likewise, except for an inverse relation between flow rate and dissolved iron and calcium concentrations at the Oak Hill Boreholes (Spearman's $r = -0.64$ and -0.79, respectively), water quality and flow at this site were not correlated (Figure 9). In contrast, at upstream and downstream sites on the West Branch (WB1, WB2 and WB3), the pH, specific conductance and concentrations of major ions exhibited significant variations with streamflow (Figure 9). Concentrations of dissolved iron in the West Branch downstream of the Pine Knot Tunnel and Oak Hill Boreholes (WB2, WB3) decreased downstream but did not vary with streamflow (Figure 9), because increased streamflow resulted in less attenuation of dissolved iron (Figure 10), as described later.

Geochemical models of water quality

The pH increased, whereas the concentrations of iron, and, to a lesser extent, manganese and sulphate decreased in the West Branch downstream of the Pine Knot Tunnel and Oak Hill Boreholes (WB2, WB3) (Figure 10A). The increase in pH with distance along the 4950-m flow path from WB2 to WB3 resulted from the gradual degassing of dissolved CO_2 (Figure 11A), whereas the decrease in iron concentrations resulted from the gradual oxidation of ferrous iron (Fe^{II}) to ferric iron (Fe^{III}), as observed for other iron-bearing, net-alkaline waters exposed to the atmosphere (Cravotta, 2007; Geroni *et al.*, 2012). In the near-neutral pH range, the rate of iron oxidation increases exponentially with pH, and the precipitation of ferric hydroxide ($Fe(OH)_3$) or related solids tends to limit the dissolved ferric iron concentration (Bigham *et al.*, 1996; Stumm and Morgan, 1996; Dempsey *et al.*, 2001). Saturation or supersaturation of most CMD and stream water samples with respect to ferrihydrite (Figure 11E) indicates Fe^{III} precipitation is thermodynamically feasible; supersaturation may indicate transport of Fe^{III} colloids (Nordstrom, 2011). The streamflow rates at

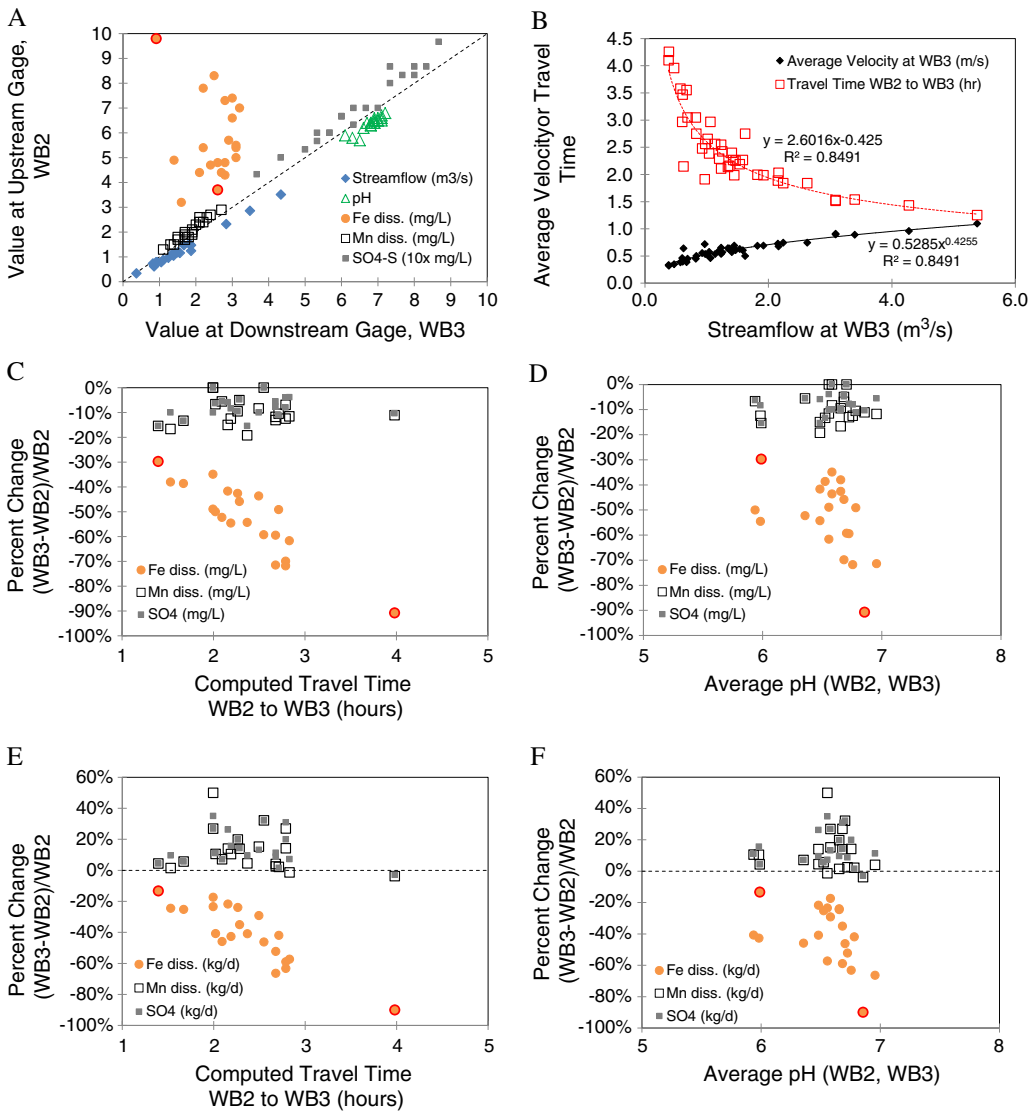

Figure 10. Relation between discharge rate, travel time, and attenuation of dissolved iron, manganese, and sulfate within the West Branch Schuylkill River below Pine Knot Tunnel and Oak Hill Boreholes, July 2005-July 2012. A, Streamflow and water quality at intermediate (WB2) and downstream (WB3) sites; B, streamflow, average flow velocity at WB3, and computed time to travel 4950 m from WB2 to WB3; C, change in concentrations from WB2 to WB3 as a function of travel time; D, change in concentrations from WB2 to WB3 as a function of pH; E, change in load from WB2 to WB3 as a function of travel time; F, change in load from WB2 to WB3 as a function of pH. Symbol for iron at low-flow and high-low "end members" highlighted by red circle. "Average pH" shown in D and F computed as the negative log of the average of $[H^+]$ concentrations at WB2 and WB3

WB2 and WB3 were similar during base flow conditions; however, during high flow conditions, streamflow at WB3 was as much as 20% larger than WB2 (Figure 10A). With increased flow rates of the West Branch, the iron removal efficiency, travel times and pH values decreased (Figure 10). The removal of dissolved iron from WB2 to WB3 was greater during base flow conditions because both the greater travel time along the flow path and the greater average pH of the stream favoured more extensive oxidation and precipitation of dissolved iron (Figures 9 (C–F)). In contrast, concentrations of dissolved manganese and sulphate were attenuated to a much lesser extent than iron. The oxidation rate of manganese is slower than that for iron and requires pH to be at least 8.5 for oxidation and precipitation to occur (Hem, 1963; Stumm and Morgan, 1996), whereas sulphate tends to be stable in surface water equilibrated with the atmosphere. Despite marginal increases in loading, manganese and sulphate concentrations decreased by as much as 20% downstream (Figures 9(C–F)). Thus, dilution by run-off or other 'clean' sources of water along the flow path could be an additional factor that affected concentrations of iron and other solutes at the sampled sites, particularly during high flow conditions.

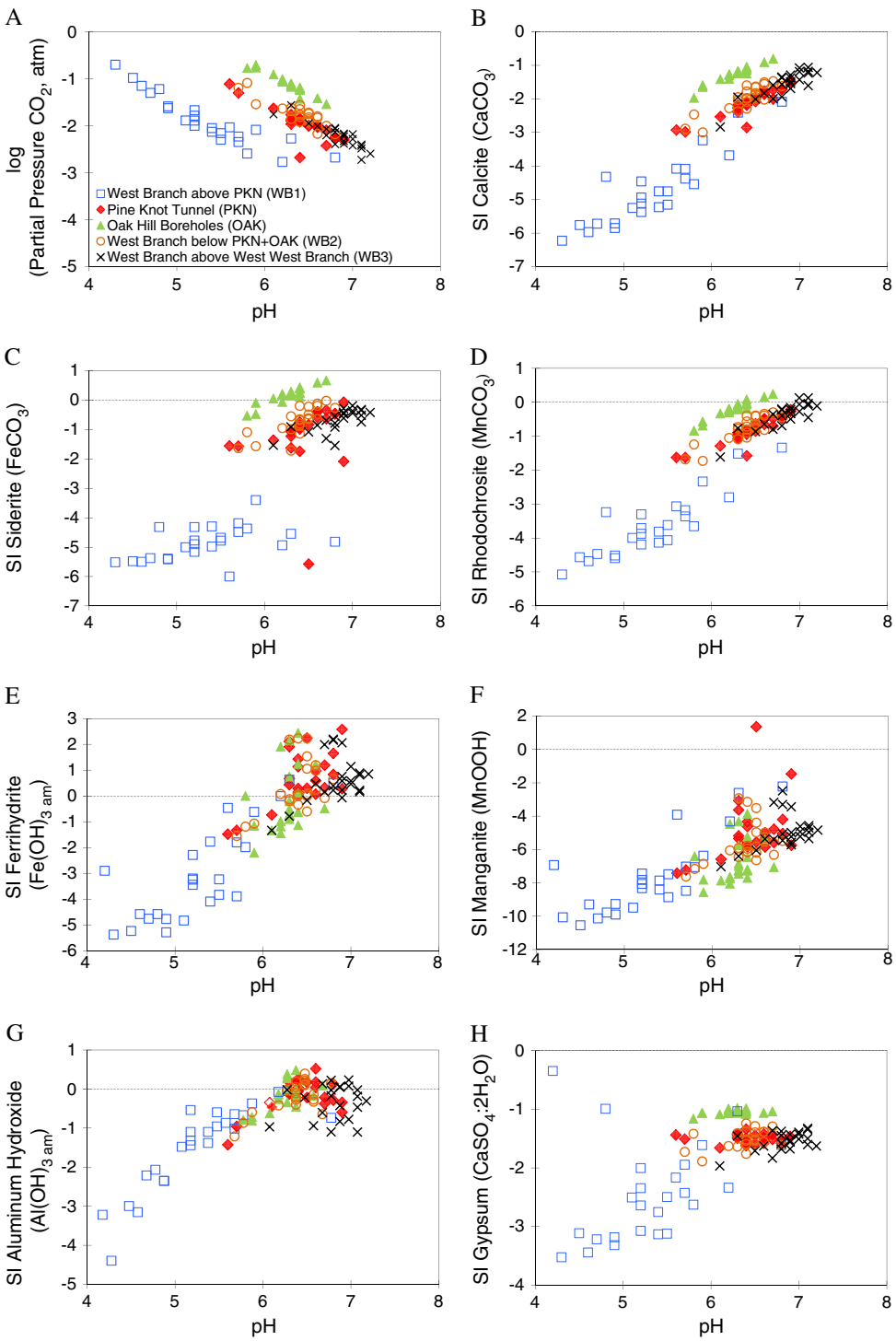

Figure 11. Relation between pH, partial pressure of CO_2 (PCO_2), and saturation index (SI) values of selected minerals for the West Branch above Pine Knot Tunnel (WB1), Pine Knot Tunnel (PKN), Oak Hill Boreholes (OAK), and West Branch below Oak Hill Boreholes at intermediate (WB2) and downstream (WB3) sites, July 2005-July 2012. Values of PCO_2 and SI computed with PHREEQC (Parkhurst and Appelo, 1999)

Geochemical mixing and mass balance models were developed using PHREEQC (Parkhurst and Appelo, 1999) to quantify important hydrochemical processes affecting water quality at the sites sampled. One of the issues considered was the potential for 'streambed leakage' to the underground mines to affect the mine discharge quality. Another issue was the magnitude of effects of geochemical reactions, with and without

dilution, on the attenuation of metals within the West Branch during low flow and high flow conditions. The application of mixing models to evaluate these issues was supported by the observation of site-specific geochemical trends as a function of flow rate (Figure 9) or pH (Figure 11), which implied different origins of the water samples during low flow and high flow conditions (end members). The model results are summarised later.

Pine Knot Tunnel discharge at high flow. The water quality discharged from the Pine Knot Tunnel (PKN_AMD) at high flow is hypothesised to be a mixture of the groundwater discharged at base flow, which has relatively constant quality, plus variable contributions of low pH, low ionic strength run-off originating as streambed leakage and/or diffuse recharge. On 24 September 2008, the Pine Knot Tunnel was sampled during extreme low flow conditions (low flow end member; 20080924) when the discharge was 0.25 m^3/s (Figure 8). On 12 March 2010–16 March 2010 (high flow end member; 20100316), the flow rate of the Pine Knot Tunnel nearly doubled, from 0.57 to 1.08 m^3/s (Figure 8). To obtain this high flow end member, the geochemical models considered mixing of the low flow end member with run-off that infiltrated to the mine. The run-off composition was estimated as a flow weighted mixture of compositions of upstream tributaries sampled during a synoptic survey of flow loss from the unmined headwaters to the mined area overlying the Pine Knot Mine on 18 July 2006 (Cravotta and Nantz, 2008). These tributaries had very low solute concentrations (SC, 21–46 μS/cm; pH, 4.5–5.1) and could be characterised as acidic precipitation that had minimal interaction with silicate and carbonate minerals. Thus, models also considered rainfall and evaporated rainfall (75% water loss) as the starting run-off compositions.

The high flow end member (20100316) composition was obtained with the models by diluting the low flow end member (20080924) with 6.8–18.1% 'run-off' (rainfall or flow weighted mix of tributary samples 20060718). The run-off and corresponding base flow fractions estimated by solute mass balance were consistent with estimates by hydrograph separation for this date and the numerical simulations of transient high flow, groundwater discharge conditions for May 2012, discussed later. The estimated mixing volumes and geochemical reactions were similar for different run-off compositions considered. The indicated reactions included the ingassing of O_2, oxidation of organic matter, dissolution of pyrite (FeS_2) or copiapite [$Fe_3(SO_4)_2{:}9H_2O$)], dissolution of Mn-siderite ($Fe_{0.95}Mn_{0.05}CO_3$) and chlorite [$Mg_5Al_2Si_3O_{10}(OH)_8$], plus precipitation of ferrihydrite [$Fe(OH)_3$] and $Al(OH)_3$ (with or without dissolution of calcite ($CaCO_3$), dolomite [$CaMg(CO_3)_2$], and/or halite (NaCl) and precipitation of quartz (SiO_2)). Quartz precipitation is used in the mass balance models as a proxy for removal of silicon by various possible precipitation and coprecipitation processes involving amorphous or poorly crystalline silica, iron oxide and aluminosilicate (clay) minerals. On the basis of computed saturation indices (Figure 11), the indicated reactions are thermodynamically feasible and may take place along the flow path as diffuse recharge or streambed seepage infiltrates to the mine pool or as the groundwater flows through the tunnel network to the surface. The reaction of pyrite or copiapite (representing stored pyrite oxidation products in soluble, solid form) is consistent with infiltrating water or rising groundwater reacting with 'acid-producing' minerals along the flow path as described by Cravotta (1994) and Perry (2001).

West Branch below Pine Knot Tunnel and Oak Hill Boreholes, near mid-point of watershed. The water quality at the intermediate streamwater sampling point on West Branch (WB2) below AMD inflows from the Pine Knot Tunnel and Oak Hill Boreholes was modelled as a flow weighted mixture of the low flow (20080924) or high flow (20100316) end members for West Branch above Pine Knot Tunnel (WB1), the Pine Knot Tunnel (PKN_AMD) and the Oak Hill Boreholes (OAK_AMD). Mass balance was achieved by degassing of CO_2 and precipitation of $Al(OH)_3$ (with or without precipitation of ferrihydrite, and/or quartz). The geochemical processes identified in these models may take place in the stream channel, particularly at the confluence of mixing waters. Although no data are available on the composition of precipitates, the results are consistent with anecdotal observations. During extreme low flow conditions, white precipitate that was presumed to be Al-rich accumulates in the channel of West Branch, below WB1, where acidic, Al-laden water flowing downstream mixes with alkaline backwater immediately upstream of the confluence with the Pine Knot Tunnel. Below the confluence with the Pine Knot Tunnel and the Oak Hill Boreholes, the streambed precipitate is stained an orange-brown that is characteristic of ochreous compounds such as ferrihydrite and goethite.

West Branch from the mid-point to the watershed outlet. The water quality at the downstream sampling point on West Branch (WB3) was modelled by starting with the water quality at the intermediate sampling point WB2 (or the mix of WB1 + PKN_AMD + OAK_AMD) and considering geochemical reactions, with or without dilution by run-off. For the low flow (20080924) end members when flows at WB2 and WB3 were comparable, geochemical mass balance reactions, alone, were indicated including ingassing of O_2, degassing of CO_2, dissolution of halite and precipitation of ferrihydrite and $Al(OH)_3$ (with or without precipitation of calcite, manganite (MnOOH) and/or quartz). For the high flow

Table V. Hydrograph-separation analysis and components of the annual hydrologic budget[a] for continuous streamflow-gauging stations in the upper Schuylkill River Basin, Schuylkill and Berks Counties, Pa., October 1, 2005 - September 30, 2010

Map ID	Gauge location	Station number	Drain age area	Mean streamflow [b]		Stream flow index [c]	Mean base flow [d]		Base flow index	Mean run-off [e]		Run-off index
			(km^2)	(m^3/s)	(cm/year)	(%)	(m^3/s)	(cm/year)	(%)	(m^3/s)	(cm/year)	(%)
WB1	WB Schuylkill River ab Pine Knot	01467688	43.0	0.451	33.1	26.9	0.346	25.4	76.7	0.105	7.7	23.3
PKN_AMD	Pine Knot Disch 500 m bl Tunnel	01467689	49.1	0.672	43.2	35.2	0.656	42.2	97.7	0.016	1.0	2.3
PKN + WB1	Pine Knot + WB ab PKN		49.1	1.123	72.2	58.7	1.002	64.4	89.2	0.121	7.8	10.8
WB3	WB Schuylkill River ab West Br	01467752	61.8	1.690	86.3	70.2	1.513	77.3	89.6	0.177	9.0	10.4
WWB	West Creek (West West Branch)	01467861	47.9	0.810	53.4	43.4	0.640	42.2	79.0	0.170	11.2	21.0
MCP	Mill Cr ab Schuylkill River	01467492	65.4	1.431	69.1	56.2	1.178	56.8	82.2	0.253	12.3	17.8
SRP	Schuylkill River ab Mill Cr	01467471	69.7	1.540	69.7	56.7	1.278	57.9	83.1	0.262	11.8	16.9
SRL	Schuylkill River at Landingville	01468500	340.9	7.785	72.1	58.7	6.277	58.1	80.6	1.508	14.0	19.4
SRB	Schuylkill River at Bern	01470500	915.3	20.891	72.0	58.6	15.158	52.3	72.6	5.733	19.7	27.4

[a] Hydrograph separation was conducted using the 'PART' computer programme (Rutledge, 1998) to divide annual streamflow into base flow and run-off contributions on the basis of daily average flow values during Water Years 2006–2010.
[b] Streamflow (yield) expressed as centimetres per year by dividing streamflow in cubic metres per second by the drainage area in square kilometres and then multiplying by the factor 3156.
[c] Streamflow index was computed as the ratio, expressed as percent, of total annual streamflow yield to average total annual rainfall of 122.9 cm/year during Water Years 2006–2010 based on total annual rainfall at local USGS streamflow gauging stations (01469500, 01470500, 01468500) and weather station 403628076134201.
[d] Base flow expressed as cubic metres per second, centimetres per year and percent of total annual streamflow (base flow index).
[e] Run-off expressed as cubic metres per second or centimetres per year was computed by subtracting the base flow from total streamflow.

(20100316) end members, the flow at WB3 (4.33 m^3/s) was larger than that at WB2 (3.51 m^3/s). Thus, flow weighted fractions of 0.81 WB2 and 0.19 'run-off' having the composition of rainfall were mixed, and mass balance reactions included degassing of CO_2, dissolution of halite, calcite, and chlorite, plus precipitation of $Al(OH)_3$ and ferrihydrite. The precipitation of $Al(OH)_3$ and ferrihydrite in both low flow and high flow models is consistent with the attenuation of iron and aluminium from upstream AMD sources over the range of flow conditions (Figures 9 and 10). The indicated dissolution reactions are consistent in the addition of 'minerals' outside the mined area including road deicing salts and limestone aggregate that are widely used in the urbanised, downstream area of the watershed (Minersville, Pottsville).

Hydrograph analysis of annual water budget

Hydrograph separation and corresponding computations of the annual hydrologic budget for each of the eight continuous gauging stations were used to evaluate potential effects of the water stored and released from the underground mines on the discharge from the Pine Knot Tunnel and streamflow characteristics in the upper Schuylkill River Basin (Table V). Although the daily average streamflow of the West Branch above the Pine Knot Tunnel (WB1) occasionally exceeded that of the Pine Knot Tunnel (PKN_AMD), particularly during high flow conditions (Figure 8), the average annual base flow yield, expressed as volume/drainage area, at WB1 (25.4 cm/year) (Table V) was less than half that estimated based on the watershed area (72.5 cm/year) and regression equations for similar size streams in Pennsylvania (Ries *et al.*, 2008). A substantial part of the base flow for this watershed was instead discharged from the Pine Knot Tunnel. Because of their shared drainage area, annual streamflow yield estimates for WB1 and PKN_AMD individually were substantially less than the values for downstream sites (Table V). Nevertheless, the combined flows of Pine Knot Tunnel and West Branch above the Pine Knot Tunnel (PKN + WB1), expressed as the yield of 71.2 cm/year for this shared area, were comparable with estimates for the downstream stations. In contrast, the West West Branch (WWB) had the smallest annual streamflow yield (52.7 cm/year), whereas the West Branch above its confluence with the West West Branch (WB3) had the greatest yield (85.3 cm/year) (Table V). This difference in yields from adjacent watersheds is indicated because the topographic watersheds used to compute streamflow yields are a poor representation of the contributing area to the WWB and WB3 stream gauges. The topographic watersheds ignore the effects of underground mining on groundwater transfers beneath topographic boundaries and associated streamflow losses

and gains. The Oak Hill and Lytle Mine (Oak Hill MCU) extend beneath the topographic divide for these neighbouring watersheds (Figure 3) and facilitate this transfer of water from the West West Branch watershed to the West Branch via the Oak Hill Boreholes discharge. In addition, recharge in the northeastern part of the West West Branch may enter interconnected mine pools of the Pine Knot MCU and discharge to the Pine Knot Tunnel.

Although the annual base flow yield estimated for the Pine Knot Tunnel (PKN_AMD) was smaller than values for most other sites, the ratio of base flow to total streamflow (base flow index) was largest for PKN_AMD (97.7%) compared with other sites (Table V), consistent with its origin as groundwater that is gradually released from the flooded underground mine complex. Thus, although flow reductions may be achieved through reductions in recharge, decreasing streambed leakage to the underground mines could have little effect on the annual water budget of PKN_AMD. Nevertheless, during large recharge events, the run-off component would increase temporarily. For example, during 16 March 2010, which is the date considered in the geochemical models to represent 'high-flow' conditions, the hydrograph separation estimates for the daily base flow and run-off contributions to the flow of the Pine Knot Tunnel were 89.5 and 10.5% of the total flow, respectively. This run-off fraction is consistent with the estimates for this date indicated by the geochemical mass balance models (6.8–18.1% run-off). Estimated annual base flow for PKN_AMD and WB1 combined (PKN + WB1) of 63.5 cm/year is comparable with values of 56.2–76.4 cm/year for the downstream stations (Table V). These base flow yields are similar to estimates reported by Risser *et al.* (2005) that are based on the long-term streamflow records for the SRL and SRB. Thus, the annual water budget for the combined PKN + WB1 is comparable with other watersheds; however, because of rapid infiltration through the mined area, the surface and groundwater interactions could be more dynamic than for nearby unmined areas.

Synoptic seepage surveys conducted in April 2004 (wet period) and July 2006 (dry period) within the drainage area above the Pine Knot Tunnel (Cravotta and Nantz, 2008) demonstrated widespread infiltration of relatively 'clean' stream water from the unmined valley sides as it flowed into the mined part of the valley overlying the Pine Knot Tunnel. On an annual basis, the discharge from the Pine Knot Tunnel restores the 'lost' water to the West Branch at their confluence, as indicated by annual yields for PKN + WB1 that are comparable with other downstream sites (Table V). However, the stream leakage losses on a given date generally would not equal the discharge from the Pine Knot tunnel because of the temporary storage and gradual release of groundwater stored in the mine pool as base flow. For example, during the synoptic seepage surveys, the total streamflow of the West Branch below the Pine Knot Tunnel was substantially less than (wet period) or greater than (dry period) two times the flow from the unmined part of the basin, which is approximately half of the watershed area.

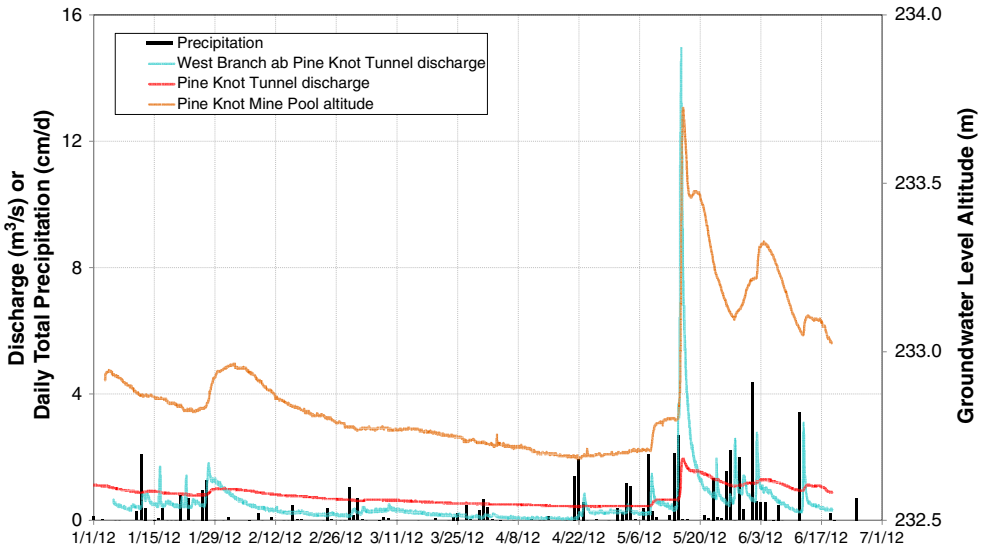

Figure 12. Temporal relations in groundwater level within Pine Knot Mine pool (hourly interval), discharge at the Pine Knot Tunnel and West Branch above Pine Knot Tunnel (15-minute interval), and corresponding daily precipitation collected by USGS at nearby rain gages, January-July 2012. Precipitation is the average of daily values for raingages maintained by USGS at Friedensburg, Pa. and at the streamgages on Schuylkill River at Tamaqua, Landingville, and Bern, Pa.

Recharge, groundwater levels and discharge of Pine Knot Tunnel

Visual evaluation of the groundwater level hydrograph for the Pine Knot Mine (available only for January–June 2012) and corresponding discharge hydrographs for the Pine Knot Tunnel and the West Branch above Pine Knot and local precipitation data (Figure 12) indicated strong temporal correlations and subtle differences that offered insights to the surface water and groundwater interactions. For example, in late January 2012, precipitation occurred as snowfall, which later melted and slowly recharged the groundwater causing a gradual increase and decrease in the Pine Knot mine pool level and tunnel discharge. For these conditions, relatively uniform recharge may have occurred throughout the area. In contrast, after a relatively dry period in early April, sustained rainfall in early to mid-May, with the greatest daily totals on 14–15 May 2012, produced complex features in the hydrographs. In response to this rainfall, the water level in the Pine Knot mine pool increased from 232.70 m at the beginning of May to a peak of 233.72 m on 16 May, declined to 233.46 m on 17 May and then increased to a subordinate peak of 233.48 m on 18 May. Various hypotheses may explain the complex trends (two peaks) in mine pool levels after the 14–15 May rainfall event. (1) Recharge water from stream leakage or mine pits reached the mine pool faster (higher permeability fractures or mine openings) than recharge through unmined soil and rock in the outer areas. The initial peak could reflect direct, rapid infiltration through mine openings and fractures to the Pine Knot Mine, and the subordinate peak could reflect delayed recharge from the outlying unmined area. (2) The subordinate peak could have resulted as groundwater levels in adjoining mine pool(s), such as the Thomaston and/or Richardson, slowly rose to an altitude where the barrier pillar(s) had been breached, and thereafter flowed to the Pine Knot mine pool. Such a breach, far from the Pine Knot tunnel, may have been a partially collapsed or blocked tunnel with limited capacity to transmit water.

Numerical model of groundwater flow

The equivalent porous media assumptions implicit in MODFLOW did not account for the local flow dynamics caused by the extreme heterogeneity of the rock matrix, fractures, and mined voids, or potential turbulent flow. Despite these limitations, MODFLOW proved useful for water budget and generalised recharge capture area calculations for the current study. Several previous studies (e.g. Rapantova *et al.*, 2007; Booth and Greer, 2011; Goode *et al.*, 2011; Uhlík and Baier, 2012) have also demonstrated the use of equivalent porous media models for regional scale simulation of flooded coal mines. The groundwater flow model evaluated the sources of water stored and discharged by the Pine Knot Mine complex and dynamic interactions among recharge, storage and discharge within the corresponding watershed area. The model was calibrated using data from the snowmelt recharge event in late January 2012. The calibrated model was used to simulate a transient high flow rainfall event in May 2012 and to simulate the spatial distribution of groundwater flow down to and within the mine complex. Direct recharge to the Pine Knot mine from surface run-off was identified as an important process during high flow events. The model simulated changes in groundwater levels, tunnel discharge and stream base flow that may result from lining of streams to reduce streambed leakage to the mines.

Estimation of hydraulic properties and recharge by model calibration. Twelve adjustable parameters were used to represent aquifer properties and recharge rates during the transient calibration period (Table VI). Model adjustments focused on parameters that caused the greatest proportional change in simulated water levels and discharge at measurement locations, which were indicated by their composite scaled sensitivities (Table VI). The overall model error changed the most for (proportional) changes in parameters with the highest composite scaled sensitivities (Hill and Tiedeman, 2007). Manually adjusted values were used for parameters for which the automated procedure yielded unrealistically low or high values and for insensitive parameters that did not substantially affect model error. Highly correlated parameters, which could not be independently calibrated, also were manually adjusted. The root mean square differences between measured and simulated values were 0.04 m for Pine Knot well water levels, 0.04 m^3/s for flow rates for Pine Knot Tunnel and the West Branch and 1.37 m for water levels in other collieries.

The conceptual model of groundwater flow in the Pine Knot area is supported by the estimated parameter values (Table VI). The highest values for HK were estimated for the mine voids, followed by the shallow surficial unit that included soil and weathered fractured rock. In the absence of mining, the underlying unweathered rock was estimated to have very low HK. The unconfined specific yield of the unmined areas was low (0.006, or 0.6%), reflecting the low storage provided by the sparse fractures in the rock. Conversely, the high specific yield of the mined areas (0.17, or 17%) indicated that the mine pools dominate groundwater storage in the area. Negligible storage was provided by the confined parts of the groundwater system. Calibration of the specific yield parameter provided an independent estimate of the mine pool storage capacity, based on measured streamflow, tunnel discharge and mine pool water level changes, rather than on estimates of coal volume removed or other geometric methods (e.g. Goode *et al.*, 2011). The

Published 2013. This article is a U.S. Government work and is in the public domain in the USA.

Table VI. Parameters of the groundwater-flow model for the Pine Knot mine complex, upper Schuylkill River Basin, Schuylkill County, Pa

Parameter ID	Description	Layers where applied	Calibration method[c]	Calibrated value	Coefficient of variation (unitless)	Composite scaled sensitivity[a] (unitless)	Largest correlation coefficient (unitless)	Most correlated parameter
				(m/day)				
HK_OB	Hydraulic conductivity (HK) of overburden	1	Ucode	5.1	0.15	0.91	−0.76	RCH_2
HK_Dist	HK of disturbed areas	2	Ucode	0.046	0.27	0.73	0.99	VANI_Void
HK_Void	HK of rock with mined voids	3, 4	Ucode	17.4	0.53	0.24	0.37	SY_Void
HK_BedR	HK of unweathered, undisturbed, unmined rock	2, 3, 4, 5	Manual	0.005		0.52	0.95	VANI_1
				(unitless)				
SY_1	Specific yield of unmined areas	1, 2	Ucode	0.006	0.09	2.50	−0.65	RCH_3
SY_Void	Specific yield of rock with mined voids	3, 4	Ucode	0.17	0.31	0.60	−0.48	VANI_Void
				(per metre)				
SS_1	Specific storage of unmined rock	2, 3, 4, 5	Manual	10^{-6}		0.06	−0.48	VANI_Void
SS_Void	Specific storage of rock with mined voids	3, 4	Manual	10^{-6}		0.00	−0.30	RCH_2
				(unitless)				
VANI_1	Ratio of horizontal to vertical HK in unmined areas	1, 2, 3, 4, 5	Manual	10		0.40	0.95	HK_BedR
VANI_Void	Ratio of horizontal to vertical HK of rock with mined voids	3, 4	Manual	1		0.81	0.99	HK_Dist
				(cm/day)				
RCH_1	Recharge rate for steady state simulation	Top active layer	Ucode	2.2	0.03	5.68	−0.42	RCH_2
RCH_2	1-day recharge rate for January snowmelt event	"	Ucode	5.3	0.04	4.97	−0.94	RCH_3
RCH_3	Recharge rate during January baseflow recession	"	Manual	0		0.14[b]	−0.94	RCH_2

[a] Composite scaled sensitivities reflect the relative change in the model error caused by a 1% change in the parameter value. Higher values correspond to parameters that the observations provide more information about (see discussion by Hill and Tiedeman, 2007).
[b] Composite scaled sensitivity computed with RCH_3 = 0.001 cm/day, to scale by one over the parameter value.
[c] Ucode, parameter estimation with UCODE-2005 (Poeter *et al*., 2005); Manual, parameter fixed by manual adjustment.

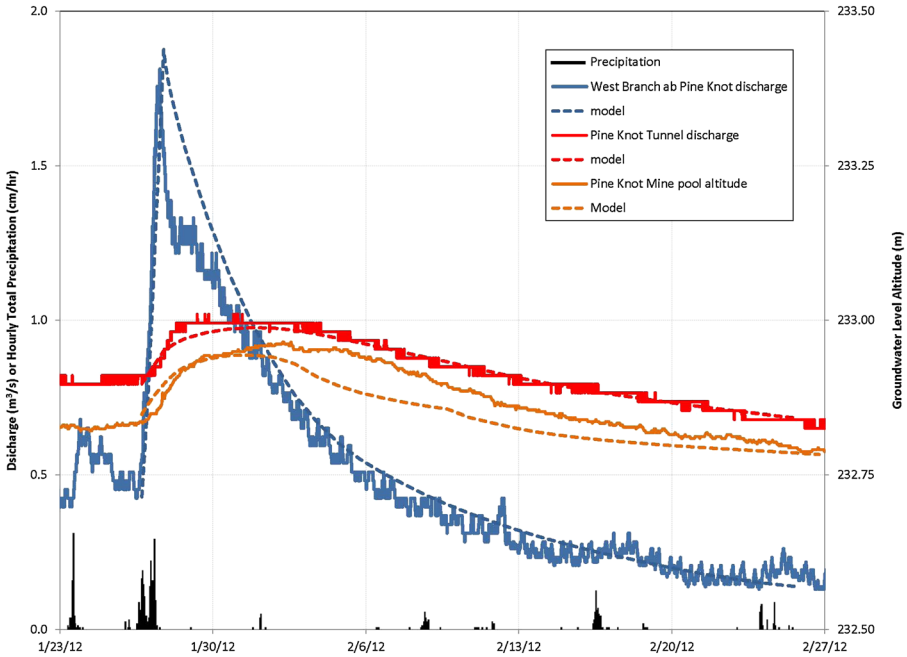

Figure 13. Average hourly precipitation, and measured and simulated water level in Pine Knot Mine, discharge at Pine Knot Tunnel and discharge at West Branch above Pine Knot Tunnel, 23 January to 27 February 2012

Table VII. Water budget for steady-state conditions simulated by use of the groundwater-flow model for the Pine Knot mine complex, upper Schuylkill River Basin, Schuylkill County, Pa.

Drainage area	West West Branch	West Branch	Mill Creek	Total
	(m3/s)			
Inflows				
Recharge	0.33	1.13	0.13	1.59
Net groundwater inflow from adjacent drainage areas	−0.09	0.10	−0.01	
Outflows				
Streams	0.24	0.43	0.11	0.78
Mine discharge	0.00	0.80	0.01	0.81

calibrated specific yield of 17% for the mined layer is intermediate between reported porosity values of 11 (Hawkins and Dunn, 2007) and 40% (Ash *et al*., 1949) for flooded underground coal mines in Pennsylvania.

Snowmelt event in January 2012. Many transient features of the observed hydrographs for the Pine Knot mine pool, Pine Knot Tunnel and West Branch above Pine Knot during and after the snowmelt recharge event in January 2012 (Figure 12) were well simulated by the calibrated model (Figure 13) despite only a limited number of parameters and a limited data set available for calibration (only one groundwater well and two streamflow gauges for a 6-month period).

Steady-state conditions. The calibrated groundwater model simulated the steady-state groundwater flow, conceptually representing long-term average conditions. The simulated water table mirrored the topography outside of the mining area. In contrast, the simulated water table within the mine pool area was relatively flat, reflecting the high HK of the mine voids. The water table above the Glendower mine pool was lower than that in the rest of the West West Branch watershed and the mine pool drained water from the West West Branch drainage area into the West Branch drainage area, through the Glendower mine pool. The water table was locally higher above the low HK barriers between the mine pools, and near losing sections of streams.

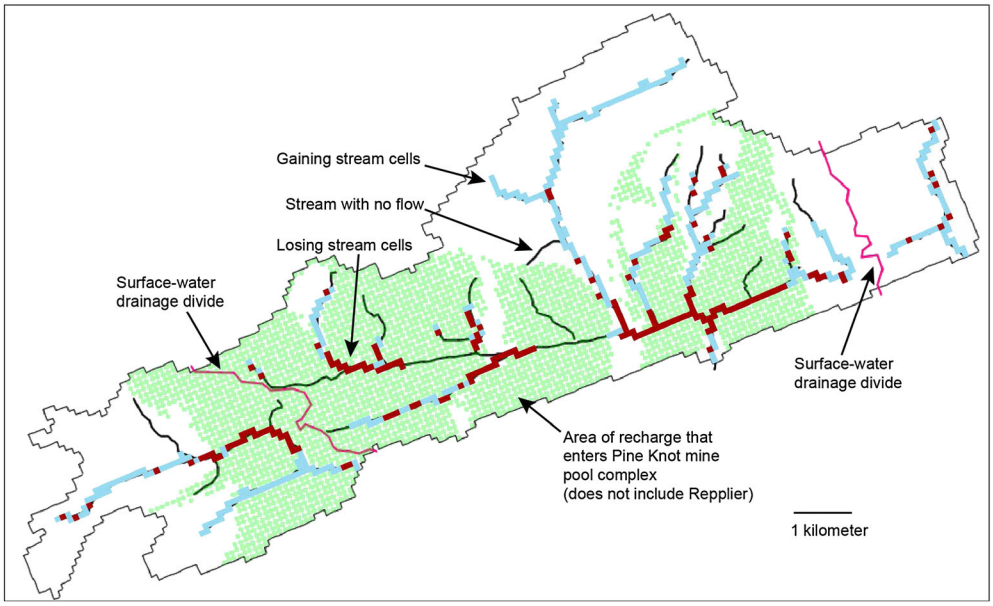

Figure 14. Simulated source areas of recharge to the Pine Knot mine pool complex and gaining and losing model stream cells under steady-state conditions

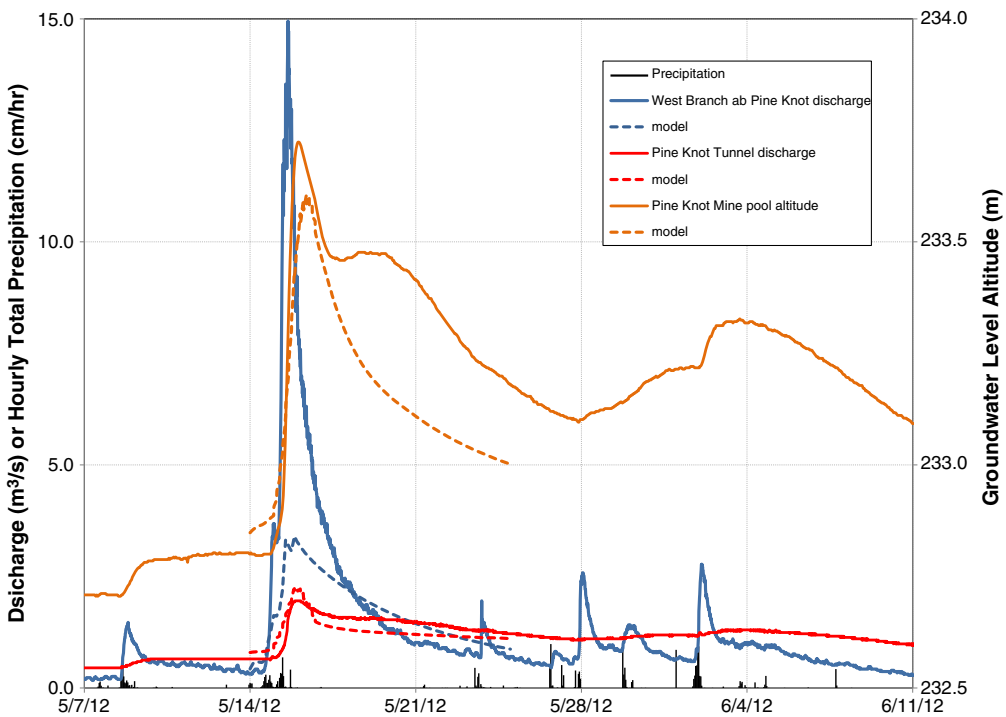

Figure 15. Average hourly precipitation, and measured and simulated water level in Pine Knot mine, discharge at Pine Knot Tunnel and discharge at West Branch above Pine Knot Tunnel, 7 May to 11 June 2012, with direct recharge to Pine Knot mine

The steady-state water budget for the separate drainage areas (West Branch, West West Branch and Mill Creek) within the model area was computed by using the base case calibrated model (Table VII). The steady-state conditions correspond to the period prior to the snowmelt event in January 2012, and these conditions may have been somewhat wetter than the long-term average conditions. The simulated water budget components were consistent with the streamflow yield analysis (Table V). The Pine Knot Tunnel captured flow from the West West

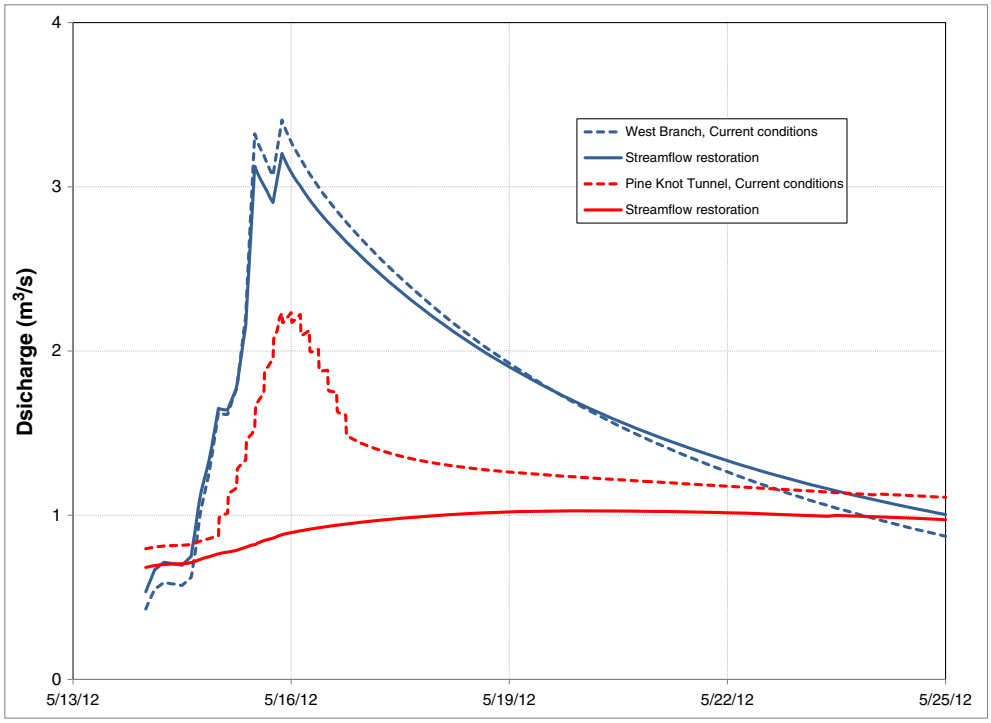

Figure 16. Groundwater model simulation of discharge at Pine Knot Tunnel and discharge at West Branch above Pine Knot Tunnel, May 13 - 25 2012 for current conditions (dashed line symbols) and streamflow restoration conditions (solid line symbols).

Branch and, to a lesser extent, the Mill Creek drainage areas and eventually discharged this flow to the West Branch (Figure 14). Much of this recharge from these areas entered the mine complex by spatially distributed recharge from the land surface and downward groundwater flow to the underlying flooded mines, and then flowed within the mine pool towards the Pine Knot Mine Tunnel, and not from surface water loss from streams directly above the Pine Knot Mine (Figure 14). The water budget indicated by the steady-state model of the current conditions (Table VII) indicates that approximately half of the 1.59 m^3/s total recharge in the model area discharges as groundwater from the Pine Knot Tunnel (listed as 0.80 m^3/s discharge from the mines to the West Branch in Table V). Because most of the recharge to the mine pool is from areas outside the stream channels, this result suggests that eliminating leakage only from the stream channels over the mines will not have a substantial effect on the long-term mine pool discharge volume or associated water levels.

Direct recharge during high flow event in May 2012. The calibrated groundwater flow model was used to simulate the mine pool level and discharge from the mine complex through the Pine Knot Tunnel, as well as base flow in the West Branch during a high flow rain event in May 2012 (Figure 15). Peak streamflow in West Branch was not well simulated by the groundwater model, because the model only accounted for the portion of streamflow resulting from discharge of groundwater to the streams (base flow) and did not include overland run-off to the stream. Additional direct recharge to model cells in layers three and four representing the Pine Knot mine was necessary to simulate the very rapid rise in the mine pool level and the tunnel discharge (Figure 15). The conceptual model is thus modified to include secondary permeability features that rapidly conducted recharge from the land surface down to the mine pool during this high flow event, but that were not a focus of recharge during the slower and smaller snowmelt recharge event. Such direct recharge can result from run-off to the mined area that is intercepted at mine openings (at coal outcrops) along the valley sides, from streamflow conveyed in intermittent reaches that do not typically convey base flow and that leak into the mines, or overbank flow outside the stream channel (flood plain) that enters mine openings or factures. The simulated amount of direct recharge was about 3% of the total event recharge.

Streamflow restoration. A hypothetical simulation of the tunnel discharge and streamflow with the elimination of streambed leakage to the Pine Knot mine pool was conducted to evaluate the effects of proposed streamflow restoration efforts. In addition to eliminating vertical streambed conductivity, the direct recharge to the mine pool during flood conditions was eliminated as part of

streamflow restoration. The simulated discharges from Pine Knot Tunnel for the May 2012 high flow event with streamflow restoration conditions were lower than those simulated for the current conditions (Figure 16). The steady-state flow from the tunnel (earliest point on graph) was simulated to be about 14% lower (0.114 m^3/s) with streamflow restoration. The reduction in the Pine Knot discharge is slightly more than the increase in the steady-state discharge from the West Branch (0.105 m^3/s), indicating that the inflow from adjacent drainage areas also was reduced a small amount because of the streamflow restoration conditions.

The simulated high flows for the West Branch were lower for the streamflow restoration conditions, although recession flows and steady-state discharge were higher than those simulated for the current conditions (Figure 16). The simulated peak flow during May 2012 was lowered by 0.2 m^3/s, or about 6%, for the project conditions with lined stream channels. Some of the stream channels that were simulated with lower conductance for the project conditions are gaining reaches in the current conditions case. Thus, lining of these reaches may have reduced groundwater discharge into the West Branch. It should be noted again that the groundwater model did not simulate the contribution of overland run-off to streamflow that may have occurred during heavy rainfall, only groundwater discharge to the streams. Thus, the actual streamflow in the West Branch, which includes flood flow or overland run-off, would be increased by the amount of direct recharge to Pine Knot Tunnel, which would be prevented by streamflow restoration. These results should be used in conjunction with compatible simulations of the West Branch streamflow that includes overland run-off during high flow events.

CONCLUSIONS

Hydrological monitoring and modelling presented in this paper offer insights on important physical and chemical interactions in historically mined areas, before and after environmental restoration. Maps showing the geographic extent and interconnection of underground mines beneath watersheds of the upper Schuylkill River Basin coupled with continuous streamflow and periodic water quality data collected along potential flow paths during 2005–2012 were useful to develop conceptual and quantitative models of surface water and groundwater interactions. Hydrograph analysis, geochemical models and steady-state and transient groundwater flow models were useful to evaluate potential effects of recharge, run-off and water–rock interactions on spatial and temporal variations in the AMD and streamwater characteristics. The methods and results generally would be applicable to other areas where surface water infiltrates to underground mines and ultimately discharges as metal-laden AMD at downstream locations.

Streamflow and water quality variability at the monitored sites in the upper Schuylkill River Basin generally could be attributed to variations in the proportions of base flow (dominated by AMD) and run-off, which were affected by infiltration and drainage characteristics of the area above a given site. Because underground mines extended beneath multiple watersheds, the recharge areas that contributed to AMD discharges were not consistent with topographic divides. Continuous streamflow gauging data for adjacent watersheds were essential for hydrograph analysis that indicated that the West West Branch had the lowest annual streamflow yield (and was least affected by AMD) compared with neighbouring gauging stations, because it loses water to the underground mines that extend beneath the topographic watershed divide and drain eastward. In contrast, the adjoining West Branch to the east had the highest yield because it gained the water lost from the West West Branch as AMD from the Pine Knot Tunnel and Oak Hill Boreholes. Hydrographs showed the AMD volume increased rapidly in response to recharge but exhibited a prolonged recession compared with nearby streams, consistent with rapid infiltration of surface water and slow release of groundwater from the mine complex.

Abandoned mine drainage discharged from Pine Knot Tunnel and Oak Hill Boreholes was the major source of loading of iron and manganese to the West Branch Schuylkill River during the study. However, the Pine Knot Tunnel had a more variable flow rate and water quality compared with the Oak Hill Boreholes. Because the water quality of these AMD sources was net-alkaline with near-neutral pH, dissolved aluminium was not elevated, and dissolved iron was predominantly ferrous. After the net alkaline AMD entered the river, the transport of iron was attenuated by oxidation and precipitation processes. The iron attenuation processes were promoted by the increase in pH along the downstream flow path that resulted from the degassing of CO_2, particularly at low flow conditions. In contrast, concentrations of sulphate and manganese generally were persistent (conservative transport) during base flow conditions and decreased with increased streamflow during high flow conditions because of dilution with low ionic strength water from acidic precipitation and run-off. Such 'dilution' during high flow conditions resulted in a decrease in transport time and a decrease in the pH of the streamwater, which resulted in less efficient oxidation and removal of iron.

Geochemical modelling demonstrated that decreased pH, decreased iron concentration and increased iron and acidity loads observed with increased discharge rates at the Pine Knot Tunnel could result from 'dilution' of the mine water with low pH, low ionic strength recharge combined with 'flushing' of accumulated acid salts (copiapite) from intermittently dry zones within or

Published 2013. This article is a U.S. Government work and is in the public domain in the USA.

overlying the mine. The combination of decreased pH and increased metals loads from the Pine Knot Tunnel during high flow conditions presents a worst case condition for passively treating the AMD because of the decreased rate of iron oxidation and less efficient metals removal at low pH, as observed downstream within the West Branch. Specifically, if aerobic ponds or wetlands were considered for treatment of marginally net alkaline AMD such as the Pine Knot Tunnel, a supplemental source of alkalinity may be needed to maintain or increase pH during high flow conditions, and/or additional storage capacity may be needed to increase detention time. These findings are consistent with previous assessments indicating that active treatment and/or streamflow restoration in headwaters areas may be necessary for effective remediation.

Despite heterogeneity of the rock matrix, fractures, and mined voids, and potential turbulent flow within the underground mines, MODFLOW proved useful for water budget and generalised recharge capture area calculations to evaluate potential for stream restoration to change the discharge characteristics of the Pine Knot Tunnel. However, the uncertainty of the model, especially at small scale and for predictive simulations, is substantial, due in part to the limited data set used for calibration. The groundwater model incorporated karst-like features with direct recharge to the mines and subsurface 'streams' across barrier pillars in the underground mine layer. The model quantified the amount of groundwater recharge to the Pine Knot mine complex from adjacent topographic watershed areas and showed that about one half of the annual recharge from mined and unmined areas was discharged to the Pine Knot Tunnel. Although the transient model demonstrated that the peak discharge from Pine Knot Tunnel during a high flow event was substantially reduced when direct recharge to the mine was eliminated by stream lining, the steady-state model showed relatively minor change in the long-term tunnel discharge with stream lining. Because the model results indicate a majority of annual recharge takes place outside the stream channels, stream restoration may not decrease the long-term AMD discharge volumes or the required size of a treatment system. Nevertheless, stream restoration could increase peak flows during storms because of increased run-off routed to streams instead of the underground mines.

By diverting run-off water to stream channels instead of mine storage, the restoration of streamflow in mined watersheds could decrease base flow and increase peak flows, which could increase potential for flooding in downstream reaches. In anticipation of such hydrological consequences, resource managers and engineers contemplating stream restoration and other alternatives for rehabilitation could incorporate mitigation for these potential effects. For example, road crossings and other structures may need to be enlarged or relocated. Additionally, water storage features such as basins or wetlands along the flood plain may be considered to compensate for decreased recharge and storage within the mine pool. Although the groundwater model calibration indicated underground storage capacity of the underground mines may be substantial, with specific yield (porosity) estimate of approximately 17%, intentionally accessing and maintaining this capacity for temporary flood storage may be difficult. Additional hydrological surveys and modelling to evaluate run-off routing, locations of rapid recharge during high flow conditions and the storage capacity of surface mine pits or other manmade structures may be considered to minimise flooding and other undesirable hydrologic effects of remediation and aquatic restoration in the upper Schuylkill River Basin and other mined watersheds.

ACKNOWLEDGMENTS

This study was conducted by the US Geological Survey (USGS) in cooperation with the Pennsylvania Department of Environmental Protection (PaDEP), the US Army Corps of Engineers (USACE), the Schuylkill Conservation District (SCD), the Schuylkill Headwaters Association, Inc. (SHA) and the US Environmental Protection Agency (USEPA). Several individuals provided critical assistance with data collection and management, including David O'Brien, Heather Eggleston, Russell Ludlow, Edward Koerkle, John Rote, and Jeffrey Bender of USGS and Michael Hewitt of the Eastern Pennsylvania Coalition for Abandoned Mine Reclamation. Although the first and second authors wrote the text for this paper, other coauthors had a significant role in data analysis and interpretation used in the paper. The authors wish to thank Stephen Peters and Rob Runkel for review comments. Any use of trade, firm or product names is for descriptive purposes only and does not imply endorsement by the US Government.

REFERENCES

Ackman TE, Jones JR. 1991. Methods to identify and reduce potential surface stream water losses into abandoned underground mines. *Environmental Geology and Water Science* **17**: 227–232.

American Public Health Association. 1998a. Acidity (2310)/Titration method. In *Standard Methods for the Examination of Water and Wastewater* (20th),Clesceri LS, Greenberg AE, Eaton AD (eds). American Public Health Association: Washington, D.C; 2.23–2.25.

American Public Health Association. 1998b. Alkalinity (2320)/titration method. In *Standard Methods for the Examination of Water and Wastewater* (20th), Clesceri LS, Greenberg AE, Eaton AD (eds). American Public Health Association: Washington, D.C; 2.26–2.28.

Ash SH, Kynor HD. 1953. Barrier pillars in the Southern Field, anthracite region of Pennsylvania. U.S. Bureau of Mines Bulletin 526, 44.

Ash SH, Whaite TH 1953. Surface water seepage into anthracite mines in the Wyoming Valley Basin Northern Field, anthracite region of Pennsylvania. U.S. Bureau of Mines Bulletin 534, 30.

Published 2013. This article is a U.S. Government work and is in the public domain in the USA.

Ash SH, Eaton WL, Hughes K, Romischer WM, Westfield J. 1949. Water pools in Pennsylvania anthracite mines. U.S. Bureau of Mines Technical Paper 727, 78.

Banta ER. 2011. ModelMate—a graphical user interface for model analysis: U.S. Geological Survey Techniques and Methods, book 6, chap. E4, 31.

Berg TM, Edmunds WE, Geyer AR, Glover AD, Hoskins DM, MacLachlan DB, Root SI, Sevon WD, Socolow AA. 1980. Geologic map of Pennsylvania. Pennsylvania Geological Survey, 4th Series, Map # 1, scale 1:2,500,000, 3 sheets.

Biesecker JE, Lescinsky JB, Wood CR. 1968. Water resources of the Schuylkill River Basin. Pennsylvania Department of Forests and Waters Water Resources Bulletin No. 3, 198.

Bigham JM, Schwertmann U, Traina SJ, Winland RL, Wolf M. 1996. Schwertmannite and the chemical modeling of iron in acid sulfate waters. *Geochimica et Cosmochimica Acta* **60**: 2111–2121.

Booth CJ, Greer CB. 2011. Modeling the hydrologic effects of longwall mining on the shallow aquifer system using MODFLOW with telescopic mesh refinement: Office of Surface Mining Applied Science Project Final Report, 95. (http://www.techtransfer.osmre.gov/NTTMainSite/appliedscience/2007/Projects/NIUBooth2007Modeling.pdf).

Brady KBC, Hornberger RJ, Fleeger G. 1998. Influence of geology on post-mining water quality-Northern Appalachian Basin. In, Brady K. B.C. Smith M.W. Schueck J.H. (eds.), *Coal Mine Drainage Prediction and Pollution Prevention in Pennsylvania*. Harrisburg, Pennsylvania Department of Environmental Protection, 5600-BK-DEP2256, 8.1–8.92.

Caruso BS, Cox TJ, Runkel RL, Velleux ML, Bencala KE, Nordstrom DK, Julien PY, Butler BA, Alpers CN, Marion A, Smith KS. 2008. Metals fate and transport modelling in streams and watersheds: state of the science and USEPA workshop review. *Hydrological Processes* **22**: 4011–4021.

Chaplin JJ, Cravotta CA III, Weitzel JB, Klemow KM. 2007. Effects of historical coal mining and drainage from abandoned mines on streamflow and water quality in Newport and Nanticoke Creeks, Luzerne County, Pennsylvania, 1999–2000. U.S. Geological Survey Scientific Investigations Report 2007–5061, 40. (http://pubs.usgs.gov/sir/2007/5061/pdf/sir2007-5061.pdf)

Cravotta CA III. 1994. Secondary iron-sulfate minerals as sources of sulfate and acidity. The geochemical evolution of acidic groundwater at a reclaimed surface coal mine in Pennsylvania. In Alpers CN, Blowes DW (eds). *Environmental geochemistry of sulfide oxidation*. Washington, D.C. American Chemical Society Symposium Series 550, 345–364. (http://pubs.acs.org/doi/pdf/10.1021/bk-1994-0550.ch023)

Cravotta CA III. 2005. Effects of abandoned coal-mine drainage on streamflow and water quality in the Mahanoy Creek Basin, Schuylkill, Columbia, and Northumberland Counties, Pennsylvania, 2001. U.S. Geological Survey Scientific Investigations Report 2004–5291, 60. 4 appendixes. (http://pubs.water.usgs.gov/sir2004-5291/)

Cravotta CA III. 2007. Passive aerobic treatment of net-alkaline, iron-laden drainage from a flooded underground anthracite mine, Pennsylvania, USA. *Mine Water and the Environment* **26**: 128–149. (http://dx.doi.org/10.1007/s10230-007-0002-8)

Cravotta CA III. 2008. Dissolved metals and associated constituents in abandoned coal-mine discharges, Pennsylvania, USA: 1. Constituent concentrations and correlations. *Applied Geochemistry* **23**: 166–202. (http://dx.doi.org/10.1016/j.apgeochem.2007.10.011)

Cravotta CA III, Kirby CS. 2004. Effects of abandoned coal-mine drainage on streamflow and water quality in the Shamokin Creek Basin, Northumberland and Columbia Counties, Pennsylvania, 1999–2001. U.S. Geological Survey Water-Resources Investigations Report 03–4311, 58. (http://pa.water.usgs.gov/reports/wrir03-4311.pdf)

Cravotta CA III, Nantz JM. 2008. Quantity and quality of stream water draining mined areas of the upper Schuylkill River basin, Schuylkill County, Pennsylvania, 2005–2007. American Society of Mining and Reclamation, 223–252. (http://www.asmr.us/Publications/Conference%20Proceedings/2008/0223-Cravotta-PA.pdf)

Cravotta CA III, Brightbill RA, Langland MJ. 2010. Abandoned mine drainage in the Swatara Creek Basin, Southern Anthracite Coalfield, Pennsylvania, USA--1. Streamwater-quality trends coinciding with the return of fish. *Mine Water and the Environment* **29**: 176–199. (http://dx.doi.org/10.1007/s10230-010-0112-6)

Cravotta CA III, Lehman WG, Blackmon MA. 2011. Data compilation and utilization for development of a prototype "qualified hydrologic unit plan" for restoration of streams degraded by acid mine drainage in the upper Schuylkill River basin, Schuylkill County, Pennsylvania, 2011: Unpublished report, 27. including 11 tables, 7 maps, and geographic information system database.

Crock JG, Arbogast BF, Lamothe PJ. 1999. Laboratory methods for the analysis of environmental samples. In, Plumlee GS, Logsdon MJ (eds.), *The Environmental Geochemistry of Mineral Deposits--Part A. Processes, techniques, and health issues*. Society of Economic Geologists, Reviews in Economic Geology, 6A, 265–287.

Dempsey BA, Roscoe HC, Ames R, Hedin R, Jeon BH. 2001. Ferrous oxidation chemistry in passive abiotic systems for the treatment of mine drainage. *Geochemistry: Exploration, Environment, Analysis* **1**: 81–88.

Eggleston JR, Kehn TM, Wood GH Jr. 1999. Anthracite. In, Schultz CH (ed.), *The geology of Pennsylvania*. Pennsylvania Geological Survey, 4th series, Special Publication 1, 458–469.

Fishman MJ, Friedman LC (eds). 1989. Methods for determination of inorganic substances in water and fluvial sediments. U.S. Geological Survey Techniques of Water-Resources Investigations, book 5, chap. A1, 545.

Foos A. 1997. Geochemical modeling of coal mine drainage, Summit County, Ohio. *Environmental Geology* **31**: 205–210.

Freeze RA, Cherry JA. 1979. Groundwater. Prentice-Hall, Inc.: Englewood Cliffs, N.J., 604.

Geroni JN, Cravotta CA III, Sapsford DJ. 2012. Evolution of the chemistry of Fe bearing waters during CO_2 degassing. *Applied Geochemistry* **27**: 2335–2347. (http://dx.doi.org/10.1016/j.apgeochem.2012.07.017)

Goode DJ, Cravotta CA III, Hornberger RJ, Hewitt MA, Hughes RE, Koury DB, Eicholtz LW. 2011. Water budgets and groundwater volumes for abandoned underground mines in the Western Middle Anthracite Coalfield, Schuylkill, Columbia, and Northumberland Counties, Pennsylvania—Preliminary estimates with identification of data needs: U.S. Geological Survey Scientific Investigations Report 2010–5261, 54. (http://pubs.usgs.gov/sir/2010/5261/)

Harbaugh AW. 2005. MODFLOW-2005, The U.S. Geological Survey modular groundwater model—the Groundwater Flow Process: U.S. Geological Survey Techniques and Methods 6-A16, variously paged.

Hawkins JW, Dunn M. 2007. Hydrologic characteristics of a 35-year-old underground mine pool. *Mine Water and the Environment* **26**: 150–159.

Hem JD. 1963. Chemical equilibria and rates of manganese oxidation: U.S. Geological Survey Water-Supply Paper **1667-A**: A1–A64.

Hill MC, Tiedeman CR. 2007. Effective groundwater model calibration: with analysis of data, sensitivities, predictions, and uncertainty. Wiley: Hoboken, N.J., 480.

Kimball BA, Broshears RE, Bencala KE, McKnight DM. 1994. Coupling of hydrologic transport and chemical reactions in a stream affected by acid mine drainage. *Environmental Science & Technology* **28**: 2065–2073.

Kirby CS, Cravotta CA III. 2005. Net alkalinity and net acidity 2: Practical considerations. *Applied Geochemistry* **20**: 1941–1964. (http://dx.doi.org/10.1016/j.apgeochem.2005.07.003)

Murley C. 2012. Oak Hill Tunnel. Unpublished images and description of the underground tunnel posted on the World Wide Web at http://www.undergroundminers.com/oakhill.html.

National Aeronautical and Space Administration. 2011. Hurricane season 2011: Lee (Gulf of Mexico). National Aeronautical and Space Administration, Hurricanes/Tropical Storm Images (http://www.nasa.gov/mission_pages/hurricanes/archives/2011/h2011_Lee.html)

National Climatic Data Center. 2012. Annual climatic summary for selected stations in Schuylkill County, PA (http://www.ncdc.noaa.gov/oa/climate/stationlocator.html)

National Weather Service. 2006. MPE rainfall totals (preliminary) June 22, 8 AM - June 30, 8 AM. National Oceanographic and Atmospheric Administration, Middle Atlantic River Forecast Center (http://www.erh.noaa.gov/er/marfc/June2006.pdf)

Niswonger RG, Prudic DE. 2005. Documentation of the streamflow-routing (SFR2) package to include unsaturated flow beneath streams—a modification to SFR1. U.S. Geological Survey Techniques and Methods 6-A13, 50.

Niswonger RG, Panday S, Ibaraki M. 2011. MODFLOW-NWT, a Newton formulation for MODFLOW-2005: U.S. Geological Survey Techniques and Methods 6-A37, 44.

Nordstrom DK. 1977. Thermochemical redox equilibria of Zobell's solution. *Geochimica et Cosmochimica Acta* **41**: 1835–1841.

Nordstrom DK. 2004. Modeling low-temperature geochemical processes. In, Drever JI. (ed.), *Surface and Ground Water, Weathering, and Soils*. Elsevier, Treatise on Geochemistry **5**: 37–72.

Nordstrom DK. 2011. Hydrogeochemical processes governing the origin, transport and fate of major and trace elements from mine wastes and mineralized rock to surface waters. *Applied Geochemistry* **26**: 1777–1791.

Parkhurst DL, Appelo CAJ. 1999. User's guide to PHREEQC (Version 2)—a computer program for speciation, batch-reaction, one-dimensional transport, and inverse geochemical calculations: U.S. Geological Survey Water-Resources Investigations Report 99–4259, 310.

Pennsylvania Department of Conservation and Natural Resources. 2008. LiDAR data of Pennsylvania: PAMAP Program, Bureau of Topographic and Geologic Survey (ftp://pamap.pasda.psu.edu/pamap_lidar/cycle1)

Pennsylvania Department of Environmental Protection. 2003. Watershed Restoration Action Strategy (WRAS) Subbasin 06A Upper Schuylkill River Watershed Schuylkill, Carbon, and Berks Counties, PA. Harrisburg, PA, Pennsylvania Department of Environmental Protection, 16. (http://www.dep.state.pa.us/dep/deputate/watermgt/wc/Subjects/Nonpointsourcepollution/Initiatives/Wraslist.htm)

Pennsylvania Department of Environmental Protection. 2010. 2010 Pennsylvania Integrated Water Quality Monitoring and Assessment Report--Clean Water Act Section 305(b) Report and 303(d) List: Harrisburg, Pa. Pennsylvania Department of Environmental Protection, 786 (http://www.portal.state.pa.us/portal/server.pt/community/water_quality_standards/10556/integrated_water_quality_report_-_2010/682562)

Perry EF. 2001. Modelling rock–water interactions in flooded underground coal mines, Northern Appalachian Basin. *Geochemistry Exploration Environment Analysis* **1**: 61–70.

Poeter EP, Hill MC, Banta ER, Mehl S, Christensen S. 2005. UCODE_2005 and six other computer codes for universal sensitivity analysis, calibration, and uncertainty evaluation. U.S. Geological Survey Techniques and Methods 6-A11, 283.

Pollock, DW. 1994. User's guide for MODPATH/MODPATH-PLOT, Version 3: a particle tracking post-processing package for MODFLOW, the U.S. Geological Survey finite-difference ground-water flow model. U.S. Geological Survey Open-File Report 94–464, 6 ch. (http://water.usgs.gov/software/MODPATH/)

Price CV, Nakagaki N, Hitt KJ, Clawges RM. 2007. Enhanced historical land-use and land-cover data sets of the U.S. Geological Survey. U.S. Geological Survey Data Series 240 [digital data] (http://pubs.usgs.gov/ds/2006/240)

Rantz SE, *et al*. 1982. Measurement and computation of streamflow. U.S. Geological Survey Water-Supply Paper 2175, 2 vols.

Rapantova N, Grmela A, Vojtek D, Halir J, Michalek B. 2007. Ground water flow modelling applications in mining hydrogeology. *Mine Water and Environment* **26**: 264–270.

Ries KG III, Guthrie JD, Rea AH, Steeves PA, Stewart DW. 2008. StreamStats--a water-resources web application: U.S. Geological Survey Fact Sheet FS 2008–3067, 8.

Risser DW, Conger RW, Ulrich JE, Asmussen MP. 2005. Estimates of groundwater recharge based on streamflow-hydrograph methods, Pennsylvania. U.S. Geological Survey Open-File Report 2005–1333, 30. (http://pa.water.usgs.gov/recharge/)

Runkel RL, Bencala KE, Kimball BA, Walton-Day K, Verplanck PL. 2009. A comparison of pre- and post-remediation water quality, Mineral Creek, Colorado. *Hydrological Processes* **23**: 3319–3333.

Rutledge AT. 1998. Computer programs for describing the recession of groundwater discharge and for estimating mean groundwater recharge and discharge from streamflow data – update. U.S. Geological Survey Water-Resources Investigations Report 98–4148, 43. (http://water.usgs.gov/ogw/part/)

Schuylkill Action Network. 2006. Schuylkill River Facts. Schuylkill Action Network, From Assessment to Protection (http://www.schuylkillactionnetwork.org/).

Schuylkill River Heritage Area. 2010. Schuylkill Canal. Schuylkill River Heritage Area (http://www.schuylkillriver.org/Schuylkill_Canal.aspx)

Stumm W, Morgan JJ. 1996. Aquatic chemistry--chemical equilibria and rates in natural waters 3rd edn, Wiley-Interscience: New York; 1022.

U.S. Environmental Protection Agency. 2009. National recommended water quality criteria—2009: U.S. Environmental Protection Agency, 22. (http://water.epa.gov/scitech/swguidance/waterquality/standards/current/upload/nrwqc-2009.pdf)

U.S. Geological Survey. 2012. Water quality samples for Pennsylvania. U. S. Geological Survey Water Resources, National Water Information System Web Interface (http://nwis.waterdata.usgs.gov/pa/nwis/qwdata)

Uhlík J, Baier J. 2012. Model evaluation of thermal energy potential of hydrogeological structures with flooded mines. *Mine Water and the Environment* **31**: 179–191.

Weather Underground, Inc. 2012. Weather station history for Frackville, Pa. (KPAFRACK2): accessed 19 September 2012 at http://www.wunderground.com/weatherstation/WXDailyHistory.asp?ID=KPAFRACK2&month=5&day=14&year=2012

Winston RB. 2009. ModelMuse - a graphical user interface for MODFLOW - 2005 and PHAST: U.S. Geological Survey Techniques and Methods 6-A29, 52. (http://pubs.usgs.gov/tm/tm6A29)

Wood GH. 1972. Geologic map of anthracite-bearing rocks in the Pottsville quadrangle, Schuylkill county, Pennsylvania. U.S. Geological Survey Miscellaneous Geologic Investigations Map I-681, scale 1:12,000

Wood GH Jr., Trexler JP, Kehn TM. 1968. Geologic maps of anthracite-bearing rocks in the west-central part of the southern Anthracite Field Pennsylvania, eastern area. U.S. Geological Survey Miscellaneous Geologic Investigations Map I-528, 6 plates

Wood GH Jr., Trexler JP, Kehn TM. 1969. Geology of the west-central part of the southern Anthracite Field and adjoining areas, Pennsylvania. U.S. Geological Survey Professional Paper 602, 150.

Wood GH Jr., Kehn TM, Eggleston JR. 1986. Deposition and structural history of the Pennsylvania Anthracite region. In Lyons PC, Rice CL (eds.), *Paleoenvironmental and tectonic controls in coal-forming basins of the United States*. Geological Society of America Special Paper **210**, 31–47.

Wyrick GG, and Borchers JW. 1981. Hydrologic effects of stress-relief fracturing in an Appalachian valley. U.S. Geological Survey Water-Supply Paper 2177, 51.

Younger PL, Wolkersdorfer C. 2004. Mining Impacts on the fresh water environment: Technical and managerial guidelines for catchment scale management. *Mine Water and the Environment* **23**: s2–s80.

Published 2013. This article is a U.S. Government work and is in the public domain in the USA.